

Sensor and Simulation Notes

Note 101

March 1970

Radiation From a Resistive Tubular Antenna Excited
by a Step Voltage

by

Lennart Marin
Northrop Corporate Laboratories
Pasadena, California

Abstract

The time dependence is calculated of the radiated field from a resistive tubular antenna excited by a step-function voltage across a circumferential delta gap. The resistive loading along the antenna is taken to be uniform and independent of frequency. Analytical expressions for the early-time and late-time behavior of the far field are derived. For intermediate time intervals the field is evaluated numerically. The radiation field of the tubular antenna differs from that of the previously treated resistive-loaded antenna mostly for small times and large resistance values.

Contents

<u>Section</u>	<u>Page</u>
I. Introduction	1
II. The Problem	3
III. The Far Field for a Step Voltage	7
IV. Some Remarks Concerning the Near Field	13
Tables	20
Figures	22
Appendices A-I	32
Figures	67
Acknowledgment	70
References	71

CLEARED
FOR PUBLIC RELEASE

PL/PA 7 JAN 97

PL 96-1170

I. Introduction

This note is a continuation of previous works^{1,2,3} in which the radiated field is calculated of an infinitely long antenna of circular cross section, either uniformly resistive-loaded or perfect conducting, excited by a step-function voltage across a delta gap.

The antenna now considered is tubular, i.e. it consists of an infinitely thin, circular cylindrical, resistive sheath. The resistance is independent of frequency and uniform along the antenna. From the mathematical viewpoint this means that the tangential electric field is continuous across the sheath whereas the tangential magnetic field is discontinuous.

The reason for studying this problem is that this model resembles more closely the actual antenna than does the previously treated antenna model, which is characterized by the boundary condition that the ratio of the tangential electric field to the tangential magnetic field at the surface of the antenna is constant. In the present model we assume a delta-generator feeding. Because of the assumed infinitesimal size of the excitation gap the radiation field has singularities. The periodic appearance of these singularities arises from the fact that the wave front is reflected at and transmitted through the resistive sheath.

In comparison to the previously treated resistive antenna² the tubular antenna shows little difference in the late-time behavior of the radiated field except for the singularities that appear in the radiation field of the tubular antenna. However, the difference in the radiated field between the two antenna models is significant for early times. For intermediate times the relative difference is small when the resistance of the sheath is small but more pronounced as the resistance per unit length is increased.

If the resistive loading is allowed to be frequency dependent as well as nonuniform one will have more flexibility in shaping the waveform of the radiation field. Of course this is a much more difficult problem to analyze and might be studied later.

In section II we formulate the problem and by making use of the saddle-point method we get an expression for the time-harmonic far field. Assuming that the generator voltage is a step-function in time we calculate in section

III the time dependence of the radiation field by performing an inverse Laplace transform of the expression deduced in section II. The time behavior of the radiated field is calculated numerically for a wide range of resistance values and is tabulated as well as graphed. Some limiting values of the solution for early time and late time are also given. Finally, in section IV some expressions for the near field are derived.

II. The Problem

Consider a conducting circular cylindrical body consisting of a thin-walled tube with radius a . The cylinder is fed by an infinitesimal gap at $z = 0$ in an ϕ -independent way. We divide space into two regions: an internal region (I) where $\rho < a$ and an external region (II) where $\rho > a$. (See figure 1.)

Assuming harmonic-time dependence ($e^{-i\omega t}$) and suppressing the time factor E_z shall satisfy

$$\Delta E_z + k_o^2 E_z = 0$$

where

$$k_o = \omega/c$$

In order to solve Maxwell's equations in (I) and (II) we will make use of the Fourier transform of the field components involved. Define

$$\hat{f}(\rho, \alpha) = \int_{-\infty}^{\infty} f(\rho, z) e^{-i\alpha z} dz$$

with the inverse transform

$$f(\rho, z) = \frac{1}{2\pi} \int_C \hat{f}(\rho, \alpha) e^{i\alpha z} d\alpha$$

where the path of integration C is shown in figure 2. Here $f(\rho, z)$ denotes an arbitrary field component.

Using the Fourier transform we get the following solution of Maxwell's equations

$$\hat{E}_z^I(\rho, \alpha) = \frac{I_o(\rho\gamma)}{I_o(a\gamma)} \hat{E}_z(a_-, \alpha), \quad \rho < a \quad (1)$$

$$\hat{E}_z^{II}(\rho, \alpha) = \frac{K_o(\rho\gamma)}{K_o(a\gamma)} \hat{E}_z(a_+, \alpha), \quad \rho > a \quad (2)$$

where $I_0(x)$ and $K_0(x)$ are modified Bessel functions. This choice of the Bessel functions is motivated by the fact that E_z must be finite for $\rho = 0$ and fulfill the radiation condition for $\rho \rightarrow \infty$. Furthermore

$$\gamma = \sqrt{\alpha^2 - k_0^2} ,$$

and a_+ denotes the outside of the wall, and a_- the inside of the wall.

For the other non-vanishing field components we have from Maxwell's equations

$$\hat{E}_\rho^I(\rho, \alpha) = \frac{-i\alpha}{\gamma} \cdot \frac{I_1(\rho\gamma)}{I_0(a\gamma)} \hat{E}_z(a_-, \alpha) , \quad \rho < a \quad (3)$$

$$\hat{E}_\rho^{II}(\rho, \alpha) = \frac{i\alpha}{\gamma} \cdot \frac{K_1(\rho\gamma)}{K_0(a\gamma)} \hat{E}_z(a_+, \alpha) , \quad \rho > a \quad (4)$$

$$\hat{H}_\phi^I(\rho, \alpha) = \frac{1}{Z_0} \cdot \frac{-ik_0}{\gamma} \cdot \frac{I_1(\rho\gamma)}{I_0(a\gamma)} \hat{E}_z(a_-, \alpha) , \quad \rho < a \quad (5)$$

$$\hat{H}_\phi^{II}(\rho, \alpha) = \frac{1}{Z_0} \cdot \frac{ik_0}{\gamma} \cdot \frac{K_1(\rho\gamma)}{K_0(a\gamma)} \hat{E}_z(a_+, \alpha) , \quad \rho > a \quad (6)$$

where Z_0 is the wave impedance of free space: $Z_0 \approx 377$ ohms.

Suppose the wall can be characterized by an impedance Z so that we have

$$E_z(a, z) = E_1(z) = Z[H_\phi^{II}(a, z) - H_\phi^I(a, z)] , \quad z \neq 0 \quad (7)$$

For a conducting wall with finite thickness Δ ($\Delta \ll a$), Z is given by $Z = \sigma^{-1} \Delta^{-1}$ where σ is the conductivity of the material of the wall.

We now go on to treat one case characterized by a slice generator at $z = 0$ having the out-put voltage V (which can be a function of frequency). Another case also characterized by a slice generator at $z = 0$ is treated in appendix I.

Suppose

$$E_z(a_+, z) = E_z(a_-, z) = -V\delta(z) + E_1(z) \quad (8)$$

the Fourier transform of which is

$$\hat{E}_z(a_+, \alpha) = \hat{E}_z(a_-, \alpha) = -V + \hat{E}_1(\alpha) \quad (9)$$

Equations (5), (6), (7), and (9) give

$$\hat{E}_1(\alpha) = \frac{\beta A(\gamma)}{\beta A(\gamma) - 1} V$$

where

$$A(\gamma) = \frac{ik_o}{\gamma} \left[\frac{K_1(a\gamma)}{K_o(a\gamma)} + \frac{I_1(a\gamma)}{I_o(a\gamma)} \right] = \frac{ik_o}{a\gamma^2 K_o(a\gamma) I_o(a\gamma)}$$

and $\beta = Z/Z_o$. Thus for the H_ϕ -component of the electromagnetic field around the antenna we have

$$\hat{H}_\phi^I(\rho, \alpha) = \frac{-ik_o}{Z_o \gamma} \frac{I_1(\rho\gamma)}{I_o(a\gamma)} \frac{1}{\beta A(\gamma) - 1} V, \quad \rho < a \quad (10)$$

$$\hat{H}_\phi^{II}(\rho, \alpha) = \frac{ik_o}{Z_o \gamma} \frac{K_1(\rho\gamma)}{K_o(a\gamma)} \frac{1}{\beta A(\gamma) - 1} V, \quad \rho > a \quad (11)$$

Introducing the current $I(z)$ on the antenna we have

$$I(z) = 2\pi a [H_\phi^{II}(a, z) - H_\phi^I(a, z)]$$

and

$$\frac{E_1(z)}{I(z)} = Z' = \frac{Z}{2\pi a}$$

Here Z' can be interpreted as the impedance per unit length of the antenna. Especially when Z is real we can introduce the resistance per unit length R . For example the time averaged ohmic loss per unit length of the antenna is given by $R|I|^2/2$. Moreover in this case we can introduce the real quantity β :

$$\beta = \frac{2\pi aR}{Z_0} \quad (12)$$

Thus, from (10) - (12) we have

$$I(z) = \frac{aV}{Z_0} \int_C \frac{A(\gamma)}{\beta A(\gamma) - 1} e^{i\alpha z} d\alpha = \frac{k_0 aV}{Z_0} \int_C \frac{1}{\beta k_0 + i\gamma^2 a K_0(a\gamma) I_0(a\gamma)} e^{i\alpha z} d\alpha$$

In the far zone where $\theta \neq 0$, (r, θ, ϕ) being the spherical coordinates with origin at the center of the antenna and $\theta = 0$ being along the positive z-axis, we can use the saddle-point method when calculating the field and get

$$H_{\phi}^{II}(r, \theta) \sim \frac{pa \sin \theta I_0(pa \sin \theta) e^{-pr}}{2Z_0 [\beta + pa \sin^2 \theta K_0(pa \sin \theta) I_0(pa \sin \theta)] r} \quad (13)$$

where $p = -ik_0$.

III. The Far Field for a Step Voltage

Let the voltage of the slice generator at $z = 0$ be a step-function in time, i.e. $v_{\text{gen}}(t) = V_0 H(t)$, where $H(t)$ is Heaviside's unit step-function. From (13) the far zone radiation field is

$$\begin{aligned} \frac{\rho Z_0 H_\phi(r, \theta, t)}{V_0} &= \frac{1}{4\pi i} \int_{c-i\infty}^{c+i\infty} \frac{a \sin^2 \theta I_0(pa \sin \theta) e^{(ct-r)p}}{\beta + pa \sin^2 \theta I_0(pa \sin \theta) K_0(pa \sin \theta)} dp \\ &= \frac{1}{4\pi i} \int_{L_1} \frac{I_0(\zeta) e^{q_\theta \zeta}}{\beta_\theta + \zeta I_0(\zeta) K_0(\zeta)} d\zeta \end{aligned} \quad (14)$$

where $q_\theta = a^{-1}(ct-r)\csc \theta$, $\beta_\theta = \beta \csc \theta$, and the path of integration, L_1 , is shown in figure 3. But, when $\text{Re}\{\beta_\theta\} > 0$, $g(\zeta, \beta_\theta) = \beta_\theta + \zeta I_0(\zeta) K_0(\zeta)$ has no zeros for $|\arg\{\zeta\}| \leq \pi/2$ (see appendix A). Thus, $L_1 = \{\zeta = \xi_0 + i\eta : \xi_0 = \text{const.} \geq 0, -\infty < \eta < \infty\}$. Here we are only interested in the case when β_θ is real and positive. Then, if z satisfies $g(z, \beta_\theta) = 0$ so does also z^* where $|z^*| = |z|$, $\arg\{z^*\} = -\arg\{z\}$.

By making use of Cauchy's integration formula and introducing the normalized time T_θ

$$T_\theta = q_\theta + 1 = \frac{ct - r + a \sin \theta}{a \sin \theta} \quad (15)$$

we can see from (14)

$$\frac{\rho Z_0 H_\phi(r, \theta, t)}{V_0} = \begin{cases} 0 & , T_\theta < 0 \\ R(T_\theta, \beta_\theta) + P(T_\theta, \beta_\theta) & , T_\theta > 0 \end{cases} \quad (16)$$

where

$$R(T_\theta, \beta_\theta) = \frac{1}{4\pi i} \int_{L_2} \frac{I_0(\zeta) e^{q_\theta \zeta}}{\beta_\theta + \zeta K_0(\zeta) I_0(\zeta)} d\zeta = \int_0^\infty f(x, \beta_\theta) e^{-T_\theta x} dx$$

$$f(x, \beta_\theta) = \frac{1}{2} \frac{x I_0^3(x) e^x}{[\beta_\theta - x I_0(x) K_0(x)]^2 + \pi^2 x^2 I_0^4(x)}$$

$$P(T_\theta, \beta_\theta) = \operatorname{Re} \left\{ \sum_{j=1}^{\infty} \frac{I_0(z_j) e^{(T_\theta-1)z_j}}{g'(z_j, \beta_\theta)} \right\}$$

$$g'(\zeta, \beta_\theta) = \frac{\partial}{\partial \zeta} g(\zeta, \beta_\theta)$$

and z_j are the zeros of $g(\zeta, \beta_\theta)$ fulfilling $\pi/2 < \arg\{z_j\} < \pi$. The path of integration, L_2 , is shown in figure 3.

$R(T_\theta, \beta_\theta)$ was evaluated numerically for a wide range of β_θ and T_θ . The zeros, z_j , were calculated numerically for different values of β_θ . For large $|z_j|$ we can find an asymptotic estimate of z_j (see appendix B). This asymptotic expression for z_j was used when $j \geq 21$.

$P(T_\theta, \beta_\theta)$ was evaluated in the following way. Put

$$P(T_\theta, \beta_\theta) = A(T_\theta, \beta_\theta) + S(T_\theta, \beta_\theta) \quad (17)$$

where

$$A(T_\theta, \beta_\theta) = \operatorname{Re} \left\{ \sum_{j=1}^{20} \frac{I_0(z_j) e^{(T_\theta-1)z_j}}{g'(z_j, \beta_\theta)} \right\}$$

$$S(T_\theta, \beta_\theta) = \operatorname{Re} \left\{ \sum_{j=21}^{\infty} \frac{I_0(z_j) e^{(T_\theta-1)z_j}}{g'(z_j, \beta_\theta)} \right\}$$

Here $A(T_\theta, \beta_\theta)$ was calculated numerically and $S(T_\theta, \beta_\theta)$ was evaluated by making use of the asymptotic expression for z_j (see appendix C). $S(T_\theta, \beta_\theta)$ is discontinuous at $T_\theta = 2n$ where n is a nonnegative integer. An investigation of the behavior of $S(T_\theta, \beta_\theta)$ around $T_\theta = 2n$ is given in appendix E. The singularities are due to the infinitesimal size of the excitation gap and their periodic appearance can be understood as the wave fronts being reflected at and transmitted through the resistive wall. The time at which the different wave fronts arrive at a distant observation point can easily be determined from figure 4.

The results of the numerical computation are presented in tables 1 and 2 and in figures 5-7.

Early-time behavior of $\rho Z_o H_\phi / V_o$

The early time in the far zone is defined by $T_\theta \ll 1$. Then we put

$$R(T_\theta, \beta_\theta) = R^{(1)}(T_\theta, \beta_\theta) + R^{(2)}(T_\theta, \beta_\theta)$$

where

$$R^{(1)}(T_\theta, \beta_\theta) = \int_0^A f(x, \beta_\theta) e^{-T_\theta x} dx$$

$$R^{(2)}(T_\theta, \beta_\theta) = \int_A^\infty f(x, \beta_\theta) e^{-T_\theta x} dx$$

We choose A such that we can use asymptotic expansion of $f(x, \beta_\theta)$ when evaluating $R^{(2)}(T_\theta, \beta_\theta)$. Then $R^{(2)}(T_\theta, \beta_\theta) \sim (\pi\sqrt{2T_\theta})^{-1}$ when $T_\theta \rightarrow 0$. $R^{(1)}(T_\theta, \beta_\theta)$ remains finite when $T_\theta \rightarrow 0$. Thus, $R(T_\theta, \beta_\theta) \sim 1/\pi\sqrt{2} \cdot 1/\sqrt{T_\theta}$ when $T_\theta \rightarrow 0$.

For $P(T_\theta, \beta_\theta)$ we have: $A(T_\theta, \beta_\theta)$ remains finite when $T_\theta \rightarrow 0$, and from appendix E it follows that

$$S(T_\theta, \beta_\theta) \sim -\frac{2\beta_\theta}{1+2\beta_\theta} \cdot \frac{1}{\pi\sqrt{2}} \cdot \frac{1}{\sqrt{T_\theta}} \quad \text{when } T_\theta \rightarrow 0$$

Thus,

$$\frac{\rho Z_o H_\phi}{V_o} = R(T_\theta, \beta_\theta) + P(T_\theta, \beta_\theta) \sim \frac{1}{1+2\beta_\theta} \cdot \frac{1}{\pi\sqrt{2}} \cdot \frac{1}{\sqrt{T_\theta}}, \quad T_\theta \rightarrow 0 \quad (18)$$

Late-time behavior of $\rho Z_o H_\phi / V_o$

The late time in the far zone is defined by $T_\theta \gg 1$.

In order to estimate $R(T_\theta, \beta_\theta)$ we make the following consideration. Put

$$e(x, \beta_\theta) = f(x, \beta_\theta) - h(x, \beta_\theta)$$

where

$$h(x, \beta_\theta) = \frac{1}{2\beta_\theta^2} \left[x - \frac{2}{\beta_\theta} x^2 \ln \frac{x\Gamma}{2} + x^2 \right], \quad \Gamma = 1.7810\dots$$

Then

$$e(0, \beta_\theta) = e'(0, \beta_\theta) = e''(0, \beta_\theta) = 0$$

The primes denote partial differentiation with respect to x . Thus,

$$\int_0^\infty e(x, \beta_\theta) e^{-T_\theta x} dx = \frac{1}{T_\theta^3} \int_0^\infty e'''(x, \beta_\theta) e^{-T_\theta x} dx$$

But

$$e'''(x, \beta_\theta) e^{-\alpha x} \in L^1(0, \infty) \quad \text{for } \alpha > 0,$$

from which it follows

$$\int_0^\infty e(x, \beta_\theta) e^{-T_\theta x} dx = O(T_\theta^{-3}) \quad \text{when } T_\theta \rightarrow \infty$$

Thus

$$R(T_\theta, \beta_\theta) \sim \int_0^\infty h(x, \beta_\theta) e^{-T_\theta x} dx = \frac{1}{2\beta_\theta^2 T_\theta^2} \left[1 + \frac{2}{T_\theta} + \frac{4}{\beta_\theta T_\theta} \ln \frac{2T_\theta}{\Gamma} - \frac{2\eta}{\beta_\theta T_\theta} \right] \quad (19)$$

where

$$\eta = \int_0^\infty u^2 \ln u e^{-u} du = 3 - 2\gamma = 1.8456\dots$$

$$\gamma = \ln \Gamma = 0.5772\dots$$

From the analysis given in appendix F it follows that $P(T_\theta, \beta_\theta)$ is negligible compared to $R(T_\theta, \beta_\theta)$ for $T_\theta \gg 1$, $T_\theta \beta_\theta > 10$ and $T_\theta \neq 2n$, n being a nonnegative integer. Thus asymptotically we have

$$\frac{\rho Z_o H_\phi}{V_o} \sim R(T_\theta, \beta_\theta)$$

where $R(T_\theta, \beta_\theta)$ is given by (19).

Large β_θ

For $\beta_\theta \gg 1$ we approximate (19) by

$$\frac{\rho Z_o H_\phi(r, \theta, t)}{V_o} \approx \frac{1}{4\pi i \beta_\theta} \int_{L_1} I_o(\zeta) e^{q_\theta \zeta} d\zeta$$

We can here choose the imaginary axis as the path of integration and get

$$\frac{\rho Z_o H_\phi(r, \theta, t)}{V_o} \approx \frac{1}{2\pi \beta_\theta} \int_0^\infty J_o(y) \cos(q_\theta y) dy = \begin{cases} \frac{1}{2\pi \beta_\theta} \frac{1}{\sqrt{2T_\theta - T_\theta^2}} & , 0 < T_\theta < 2 \\ 0 & , T_\theta > 2, T_\theta < 0 \end{cases} \quad (20)$$

Some Remarks on the Results

The results of the numerical computations are presented in tables 1 and 2 and in figures 5-7. In figure 5 the radiation field of the resistive tubular antenna is graphed for $12 < T_\theta < 120$ and $\beta_\theta = 0, 0.04, 0.1, 0.4, 1, 4, 10$. For comparison purpose the corresponding curves for the previously treated resistive antenna are also shown in figure 5. For $\beta_\theta \leq 1$ the curves for the two cases are indistinguishable but the difference among them increases as β_θ increases.

Because of the unphysical assumption of the delta-gap the far field has square-root singularities at $T_\theta = 2n$, n being a nonnegative integer. As mentioned before, these singularities can be understood as being due to the wave front being reflected at and transmitted through the resistive wall. The appearance of these singularities is most pronounced for early times (see figure 6). However, the strength of these singularities is exponentially

attenuated with T_θ , and for $T_\theta > 12$ they are very weak. In figure 5 we have made the graph of the far field a smooth curve, thereby omitting the singularities for $T_\theta = 2n$. In the curves depicted in figure 6 we have omitted the time intervals $4n \leq T_\theta < 4n + 0.01$ and $4n + 2 - 0.01 < T_\theta \leq 4n + 2$ thereby making the quantity, $\rho Z_\theta H_\phi / V_\theta$, finite. If we replaced the delta-gap by a feeding gap of finite width (d) the radiation field would be finite for all times. However, if $d/a \ll 1$ maxima and minima would occur in the radiation field around $T_\theta = 2n$. These extreme values will be more pronounced the smaller d/a is and the smaller n is.

For $T_\theta < 0.2$ the radiation field can be calculated from the asymptotic expression (18). For $T_\theta > 1000$ and $\beta_\theta T_\theta > 100$ the asymptotic expression (19) is valid.

IV. Some Remarks Concerning the Near Field

As in section III we here assume that the driving function is a step-function in time, i.e. $v_{\text{gen}}(t) = V_0 H(t)$. By taking an inverse Laplace transform of the time-harmonic expression (11) we get

$$\frac{z_0}{V_0} H_{\phi}^{\text{II}}(\rho, z, t) = f(\rho, z, t) = \frac{1}{2\pi i} \int_{C_p} e^{pct} dp \frac{1}{2\pi} \int_{C_{\alpha}} \frac{a\gamma I_0(a\gamma) K_1(\rho\gamma) e^{i\alpha z}}{\beta p + a\gamma^2 I_0(a\gamma) K_0(a\gamma)} d\alpha \quad (21)$$

where $\gamma = \sqrt{\alpha^2 + p^2}$, and the paths of integration, C_p and C_{α} , are shown in figures 2 and 8. From this expression it follows that $f(\rho, z, t)$ is an even function of z . Thus there is no loss in generality to consider only the case $z \geq 0$.

Introduce now the transformation $\gamma = \sqrt{\alpha^2 + p^2}$ or $\alpha = \sqrt{\gamma^2 - p^2}$. The function $\sqrt{\gamma^2 - p^2}$ is multivalued and can be made single-valued by introducing branch cuts at $\gamma = \pm p$.

The path of integration in the γ -plane, C_{γ} , which is the image of C_{α} under the given transformation, must be such that when $\gamma \in C_{\gamma}$, i.e. γ belongs to C_{γ} , we have

1. $\alpha = \sqrt{\gamma^2 - p^2}$ is real
2. $\text{Re}\{\gamma\} \geq 0$
3. $\text{Im}\{\gamma\} \geq 0$

Introducing the notations: $\gamma_r = \text{Re}\{\gamma\}$ and $\gamma_i = \text{Im}\{\gamma\}$, and similarly for p we arrive at the following conditions that determine $C_{\gamma}(p)$

$$\gamma_r \gamma_i = p_r p_i \quad (22)$$

$$\gamma_r^2 - \gamma_i^2 - p_r^2 + p_i^2 \geq 0 \quad (23)$$

$$\gamma_r \geq 0 \quad (24)$$

This means that $C_Y(p)$ must coincide with the part of the hyperbola (22) where (23) and (24) are satisfied. (See figure 9). But α is positive and real on one part of $C_Y(p)$ and negative and real on the other part. This can be taken into account in the following way: introduce a branch-cut for $\alpha = \sqrt{\gamma^2 - p^2}$ starting from the branch-point $\gamma = p$ to infinity along the part of the hyperbola (22) where (23) and (24) are satisfied. Then α differs only in sign on the two different sides of the cut. Let one part of $C_Y(p)$ be above the branch-cut and the other part below it. (See figure 9). Moreover introduce a branch-cut from $\gamma = -p$ to infinity along the part of the hyperbola (22) fulfilling (23) and $\gamma_r < 0$. (See figure 9). We then define our Riemann-sheet for γ as the γ -plane with the two branch-cuts described and $\text{Im}\{\sqrt{\gamma^2 - p^2}\} \geq 0$. This means that $(\sqrt{\gamma^2 - p^2})_{\gamma=0} = ip$ as $\text{Re}\{p\} \geq 0$ when $p \in C_p$ and in general $\sqrt{\gamma^2 - p^2} = i\sqrt{p^2 - \gamma^2}$.

Here we want to point out that $\gamma = 0$ is a branch-point for the Bessel-functions involved. The corresponding branch-cut can be drawn from the origin to infinity along the negative real axis.

From the above considerations we change the integration variable α to γ and obtain from (21)

$$f(p, z, t) = \frac{1}{2\pi i} \int_{C_p} e^{pct} dp \frac{1}{2\pi i} \int_{C_Y(p)} \frac{a\gamma^2 I_0(a\gamma) K_1(\rho\gamma) e^{-z\sqrt{p^2 - \gamma^2}}}{[\beta p + a\gamma^2 I_0(a\gamma) K_0(a\gamma)] \sqrt{p^2 - \gamma^2}} d\gamma$$

Let p_0 be such that all singularities of

$$\int_{C_Y(p)} \frac{a\gamma^2 I_0(a\gamma) K_1(\rho\gamma) e^{-z\sqrt{p^2 - \gamma^2}}}{[\beta p + a\gamma^2 I_0(a\gamma) K_0(a\gamma)] \sqrt{p^2 - \gamma^2}} d\gamma$$

are to the left of p_0 . Then $p_r > p_0$ when $p_r \in C_p$. From appendix G it then follows that for β real and positive and by choosing p_r arbitrarily large $\beta p + a\gamma^2 I_0(a\gamma) K_0(a\gamma)$ has no zeros for $\text{Re}\{\gamma\} > 0$. This means that we can deform $C_Y(p)$ into Γ_Y parallel to the imaginary axis with $0 < \text{Re}\{\gamma\} < \text{Re}\{p\}$ when $\gamma \in \Gamma_Y$ and $p \in C_p$ (see figure 9). But Γ_Y is contrary to $C_Y(p)$ independent

of p . Interchanging the order of integration we have

$$f(\rho, z, t) = \frac{1}{2\pi i} \int_{\Gamma_\gamma} a\gamma^2 I_0(a\gamma) K_1(\rho\gamma) d\gamma \frac{1}{2\pi i} \int_{C_p} \frac{e^{pct} e^{-z\sqrt{p^2 - \gamma^2}}}{[\beta p + h(\gamma)] \sqrt{p^2 - \gamma^2}} dp \quad (25)$$

where $h(\gamma) = a\gamma^2 I_0(a\gamma) K_0(a\gamma)$. From the well known results⁸

$$\frac{1}{2\pi i} \int_{C_p} \frac{e^{pct} e^{-z\sqrt{p^2 - \gamma^2}}}{[p + \beta^{-1} h(\gamma)] \sqrt{p^2 - \gamma^2}} dp = \begin{cases} 0 & , \quad ct < z \\ c \int_{z/c}^t e^{-\beta^{-1} h(\gamma) c(t-\tau)} I_0(\gamma \sqrt{c^2 \tau^2 - z^2}) d\tau & , \quad ct > z \end{cases}$$

(25) reduces for $ct > z$ to

$$f(\rho, z, t) = \frac{c}{2\pi i \beta} \int_{\Gamma_\gamma} a\gamma^2 I_0(a\gamma) K_1(\rho\gamma) d\gamma \int_{z/c}^t e^{-\beta^{-1} h(\gamma) c(t-\tau)} I_0(\gamma \sqrt{c^2 \tau^2 - z^2}) d\tau$$

Interchanging the order of integration we get

$$f(\rho, z, t) = \frac{c}{2\pi i \beta} \int_{z/c}^t d\tau \int_{\Gamma_\gamma} a\gamma^2 I_0(a\gamma) K_1(\rho\gamma) e^{-\beta^{-1} h(\gamma) c(t-\tau)} I_0(\gamma \sqrt{c^2 \tau^2 - z^2}) d\gamma \quad (26)$$

The integrand has no singularities in the γ -plane except for the branch-cut from the origin to infinity along the real negative axis. Thus we can choose

Γ_γ as the imaginary axis.

For $|\gamma| \rightarrow \infty$ and $\text{Re}\{\gamma\} > 0$ we have

$$a\gamma^2 I_0(a\gamma) K_1(\rho\gamma) e^{-\beta^{-1} h(\gamma) c(t-\tau)} I_0(\gamma \sqrt{c^2 \tau^2 - z^2}) \sim \sqrt{\frac{\gamma}{8\pi \sqrt{c^2 \tau^2 - z^2}}} e^{-\gamma(\rho - a + 0.5\beta^{-1} c(t-\tau) - \sqrt{c^2 \tau^2 - z^2})},$$

Thus $f(\rho, z, t) = 0$ for $ct < \sqrt{(\rho - a)^2 + z^2}$ when $\text{Re}\{\beta\} > 0$.

Partial integration of (26) gives

$$f(\rho, z, t) = \frac{1}{2\pi i} \int_{\Gamma_Y} \frac{K_1(\rho\gamma)}{K_0(a\gamma)} I_0(\gamma\sqrt{c^2 t^2 - z^2}) d\gamma +$$

$$\frac{c^2}{2\pi i} \int_{\Gamma_Y} \frac{\gamma K_1(\rho\gamma)}{K_0(a\gamma)} d\gamma \int_{c^{-1}\sqrt{(\rho-a)^2 + z^2}}^t e^{-\beta^{-1}h(\gamma)c(t-\tau)} \frac{\tau}{\sqrt{c^2 \tau^2 - z^2}} I_1(\gamma\sqrt{c^2 \tau^2 - z^2}) d\tau \quad (27)$$

The first integral, f_0 , represents the field from a perfect conducting cylinder and has been evaluated earlier³. The second integral, k , can be transformed into

$k(\rho, z, t)$

$$= \frac{1}{2\pi i} \int_{-i\infty}^{+i\infty} \frac{\gamma K_1(\rho\gamma)}{K_0(a\gamma)} d\gamma \int_{\rho-a}^t I_1(u\gamma) e^{-\beta^{-1}h(\gamma)(ct - \sqrt{u^2 + z^2})} du$$

$$= \frac{1}{2\pi i a^2} \int_0^\infty \frac{\sigma [J_1(\sigma\rho/a) + iY_1(\sigma\rho/a)]}{J_0(\sigma) + iY_0(\sigma)} d\sigma \int_{\rho-a}^t J_1(\sigma u/a) e^{\ell(\sigma, u)} du$$

$$- \frac{1}{2\pi i a^2} \int_0^\infty \frac{\sigma [J_1(\sigma\rho/a) - iY_1(\sigma\rho/a)]}{J_0(\sigma) - iY_0(\sigma)} d\sigma \int_{\rho-a}^t J_1(\sigma u/a) e^{\ell^*(\sigma, u)} du$$

$$= \frac{1}{\pi a^2} \int_0^\infty \frac{\sigma [J_0(\sigma)Y_1(\sigma\rho/a) - Y_0(\sigma)J_1(\sigma\rho/a)]}{J_0^2(\sigma) + Y_0^2(\sigma)} d\sigma \int_{\rho-a}^t J_1(\sigma u/a) e^{\ell_1(\sigma, u)} \cos[\ell_2(\sigma, u)] du$$

$$+ \frac{1}{\pi a^2} \int_0^\infty \frac{\sigma [J_0(\sigma)J_1(\sigma\rho/a) + Y_0(\sigma)Y_1(\sigma\rho/a)]}{J_0^2(\sigma) + Y_0^2(\sigma)} d\sigma \int_{\rho-a}^t J_1(\sigma u/a) e^{\ell_1(\sigma, u)} \sin[\ell_2(\sigma, u)] du, \quad (28)$$

where

$$t^* = \sqrt{c^2 t^2 - z^2}$$

$$\ell(\sigma, u) = \ell_1(\sigma, u) + i\ell_2(\sigma, u)$$

$$\ell_1(\sigma, u) = -\frac{\pi\sigma^2}{2a\beta} J_0(\sigma) Y_0(\sigma) (ct - \sqrt{u^2+z^2})$$

$$\ell_2(\sigma, u) = \frac{\pi\sigma^2}{2a\beta} J_0^2(\sigma) (ct - \sqrt{u^2+z^2})$$

and the star denotes the complex conjugate value, that is, ℓ^* is the complex conjugate of ℓ .

For β small we have

$f(\rho, z, t)$

$$\begin{aligned} &= \frac{1}{2\pi i} \int_{\Gamma_Y} a_Y^2 I_0(a_Y) K_1(\rho Y) dY \frac{1}{2\pi i} \int_{C_p} \frac{e^{pct} e^{-z\sqrt{p^2-\gamma^2}}}{[\beta p+h(\gamma)]\sqrt{p^2-\gamma^2}} dp \\ &\approx \frac{1}{2\pi i} \int_{\Gamma_Y} \frac{K_1(\rho Y)}{K_0(a_Y)} dY \frac{1}{2\pi i} \int_{C_p} \frac{e^{pct} e^{-z\sqrt{p^2-\gamma^2}}}{\sqrt{p^2-\gamma^2}} dp \\ &- \frac{\beta}{2\pi i} \int_{\Gamma_Y} \frac{K_1(\rho Y)}{a_Y^2 I_0(a_Y) K_0(a_Y)} dY \frac{1}{2\pi i} \int_{C_p} \frac{pe^{pct} e^{-z\sqrt{p^2-\gamma^2}}}{\sqrt{p^2-\gamma^2}} dp \end{aligned}$$

$$= f_0(\rho, z, t) - \begin{cases} 0, & ct < \sqrt{(\rho-a)^2+z^2} \\ \frac{\beta}{2\pi i} \frac{ct}{\sqrt{c^2t^2-z^2}} \int_{\Gamma_Y} \frac{K_1(\rho Y) I_1(\gamma\sqrt{c^2t^2-z^2})}{a_Y I_0(a_Y) K_0^2(a_Y)} dY, & ct > \sqrt{(\rho-a)^2+z^2} \end{cases}$$

Thus,

$$\begin{aligned}
k(\rho, z, t) \approx k_1(\rho, z, t) &= -\frac{\beta}{2\pi i} \frac{ct}{\lambda} \int_{\Gamma'} \frac{K_1(\rho\gamma)I_1(\lambda\gamma)}{a\gamma I_0(a\gamma)K_0^2(a\gamma)} d\gamma \\
&\quad - \frac{\beta}{2\pi i} \frac{ct}{\lambda} \int_{\Gamma''} \frac{K_1(\rho\gamma)I_1(\lambda\gamma)}{a\gamma I_0(a\gamma)K_0^2(a\gamma)} d\gamma
\end{aligned} \tag{29}$$

where $\lambda = \sqrt{c^2 t^2 - z^2}$ for $\lambda > \rho - a$. The path of integration Γ' is the part of Γ_Y where $\text{Im}\{\gamma\} < 0$ and Γ'' is the part of Γ_Y where $\text{Im}\{\gamma\} > 0$. We also note that Γ' and Γ'' can be arbitrarily close to the imaginary axis.

Using the relationships $i\pi I_1(w) = -K_1(w) - K_1(we^{i\pi})$, $i\pi I_1(w) = K_1(w) + K_1(we^{-i\pi})$ we get

$$\begin{aligned}
&k_1(\rho, z, t) \\
&= -\frac{\beta}{2\pi^2} \frac{ct}{\lambda} \lim_{\epsilon \rightarrow 0} \left\{ \int_{\Gamma'_\epsilon} \frac{K_1(\rho\gamma)K_1(\lambda\gamma)}{a\gamma I_0(a\gamma)K_0^2(a\gamma)} d\gamma + \int_{\Gamma'_\epsilon} \frac{K_1(\rho\gamma)K_1(\lambda\gamma e^{i\pi})}{a\gamma I_0(a\gamma)K_0^2(a\gamma)} d\gamma \right\} \\
&\quad + \frac{\beta}{2\pi^2} \frac{ct}{\lambda} \lim_{\epsilon \rightarrow 0} \left\{ \int_{\Gamma''_\epsilon} \frac{K_1(\rho\gamma)K_1(\lambda\gamma)}{a\gamma I_0(a\gamma)K_0^2(a\gamma)} d\gamma + \int_{\Gamma''_\epsilon} \frac{K_1(\rho\gamma)K_1(\lambda\gamma e^{-i\pi})}{a\gamma I_0(a\gamma)K_0^2(a\gamma)} d\gamma \right\}
\end{aligned}$$

The paths of integration, Γ'_ϵ and Γ''_ϵ , are shown in figure 10. Next we use Cauchy's integral theorem on the contours: $\Gamma'_\epsilon + \ell_\epsilon^4 + R_\epsilon^+ + R_4$, $\Gamma'_\epsilon + \ell_\epsilon^3 + R_\epsilon^+ + R_3$, $\Gamma''_\epsilon + R_1 + (-R_\epsilon^+) + \ell_\epsilon^1$, $\Gamma''_\epsilon + R_2 + R_\epsilon'' + \ell_\epsilon^2$ (see figure 10). From the asymptotic expressions of I_0 , K_0 , K_1 it is easy to show that the integrals over the infinite quarter circles R_k ($k = 1, 2, 3, 4$) vanish for $c^2 t^2 > (\rho - a)^2 + z^2$.

Using $K_\mu(we^{im\pi}) = e^{-im\mu\pi} K_\mu(w) - i\pi \sin(m\mu\pi) \text{csc}(\mu\pi) I_\mu(w)$ and $I_\mu(we^{im\pi}) = e^{im\mu\pi} I_\mu(w)$ we get

$$k_1(\rho, z, t) = k_1^I(\rho, z, t) + k_1^{II}(\rho, z, t) \tag{30}$$

Here k_1^I is given by

$$\begin{aligned}
k_1'(\rho, z, t) &= \frac{\beta c t}{\pi^2 a \lambda} \lim_{\epsilon \rightarrow 0} \left\{ \int_{\epsilon}^{\infty} \frac{K_1(\sigma \rho/a) K_1(\sigma \lambda/a)}{\sigma I_0(\sigma) K_0^2(\sigma)} d\sigma \right. \\
&\quad - \frac{1}{2} \int_{\epsilon}^{\infty} \frac{[K_1(\sigma \rho/a) - i\pi I_1(\sigma \rho/a)] K_1(\sigma \lambda/a)}{\sigma I_0(\sigma) [K_0(\sigma) + i\pi I_0(\sigma)]^2} d\sigma - \frac{1}{2} \int_{\epsilon}^{\infty} \frac{[K_1(\sigma \rho/a) + i\pi I_1(\sigma \rho/a)] K_1(\sigma \lambda/a)}{\sigma I_0(\sigma) [K_0(\sigma) - i\pi I_0(\sigma)]^2} d\sigma \\
&\quad \left. + \frac{a}{\epsilon^2 \rho \lambda} \int_0^{\pi} \frac{\ln^2 [2\Gamma^{-1} \epsilon e^{-i\phi}] e^{i(2\phi+\pi/2)} + \ln^2 [2\Gamma^{-1} \epsilon e^{i\phi}] e^{-i(2\phi+\pi/2)}}{|\ln [2\Gamma^{-1} \epsilon e^{-i\phi}]|^4} d\phi \right\} \quad (31)
\end{aligned}$$

and it is easy to show that the integrals together gives a finite contribution when ϵ tends to zero. This is obvious because the magnitude of the integrand of equation (29) is asymptotically given by $|\gamma|^{-1} \ln^{-2} |\gamma|$ for $|\gamma| \ll 1$.

We now examine k_1'' in (30).

$$\begin{aligned}
k_1''(\rho, z, t) &= \frac{\beta c t}{\pi a \lambda} \sum_{j=1}^{\infty} \left\{ \frac{K_1(\xi_j \rho/a e^{-i\pi/2}) K_1(\xi_j \lambda/a e^{i\pi/2})}{\xi_j I_1(\xi_j e^{-i\pi/2}) K_0^2(\xi_j e^{-i\pi/2})} \right. \\
&\quad \left. + \frac{K_1(\xi_j \rho/a e^{i\pi/2}) K_1(\xi_j \lambda/a e^{-i\pi/2})}{\xi_j I_1(\xi_j e^{i\pi/2}) K_0^2(\xi_j e^{i\pi/2})} \right\} \\
&= \frac{2\beta c t}{\pi a \lambda} \sum_{j=1}^{\infty} \frac{J_1(\xi_j \rho/a) Y_1(\xi_j \lambda/a) - J_1(\xi_j \lambda/a) Y_1(\xi_j \rho/a)}{\xi_j J_1(\xi_j) Y_0^2(\xi_j)} \quad (32)
\end{aligned}$$

An evaluation of the sum is given in appendix H. From this analysis it follows that $k_1''(\rho, z, t)$ has singularities at $c^2 t^2 = [\rho + (2n-1)a]^2 + z^2$, n nonnegative integer. These singularities are due to partial transmissions and reflexions of the wave front at the resistive wall. In general one can show from (25) that $f(\rho, z, t)$ has singularities at $c^2 t^2 = [\rho + (2n-1)a]^2 + z^2$.

Table 1. Values of $\frac{\rho Z_o H_o}{V_o} \times 10^2$

$T_\theta \backslash \beta_\theta$	0	.02	.03	.04	.05	.06	.07	.08	.09	.10	.20	.40	.80
.2	51.5	50.7	49.8	48.9	47.9	47.1	46.3	45.6	44.7	44.0	37.9	29.5	20.5
.4	38.3	37.3	36.6	36.0	35.4	34.7	34.2	33.6	33.0	32.4	27.9	21.8	15.2
.8	29.3	28.3	27.8	27.4	26.9	26.5	26.0	25.7	25.2	24.9	21.6	17.1	12.1
1.4	24.2	23.4	23.2	22.9	22.6	22.4	22.1	21.9	21.6	21.4	19.3	15.9	11.7
1.9	21.7	22.6	23.1	23.4	23.8	24.1	24.3	24.6	24.8	24.9	25.6	24.4	20.2
3.0	18.8	17.2	16.5	15.8	15.2	14.6	14.0	13.5	13.0	12.5	8.87	5.12	2.34
4.1	17.2	18.0	18.3	18.6	18.7	18.8	18.9	18.9	18.9	18.8	17.4	13.4	7.83
5.0	16.2	15.1	14.5	13.9	13.4	12.9	12.5	12.0	11.6	11.2	8.26	5.07	2.50
5.9	15.6	12.8	11.5	10.4	9.47	8.60	7.81	7.11	6.48	5.91	2.52	.670	.264
7.0	14.9	14.2	13.8	13.5	13.1	12.7	12.3	12.0	11.6	11.3	8.32	4.78	2.01
8.1	14.4	11.4	10.1	9.04	8.10	7.28	6.57	5.95	5.40	4.93	2.36	1.17	.683
9.0	14.1	13.0	12.4	11.9	11.4	11.0	10.5	10.1	9.68	9.29	6.28	3.23	1.22
9.9	13.8	13.8	13.7	13.5	13.2	12.9	12.6	12.2	11.8	11.5	7.95	3.86	1.27
13	13.2	11.1	10.3	9.59	8.96	8.39	7.88	7.41	6.99	6.60	4.01	1.87	.636
17	12.3	10.9	10.2	9.62	9.03	8.47	7.94	7.44	6.98	6.56	3.62	1.41	.404
23	11.6	9.61	8.81	8.08	7.42	6.83	6.30	5.81	5.37	4.98	2.49	.871	.225
29	11.1	8.43	7.51	6.74	6.08	5.52	5.03	4.60	4.22	3.88	1.84	.588	.140
35	10.7	8.46	7.55	6.64	6.02	5.39	4.83	4.35	3.92	3.54	1.47	.420	.094
45	10.4	7.33	6.35	6.54	4.87	4.29	3.80	3.38	3.01	2.69	1.01	.258	.055
55	10.2	6.62	5.62	4.83	4.18	3.64	3.18	2.78	2.45	2.16	.732	.172	.036
65	9.90	6.36	5.31	4.47	3.79	3.23	2.76	2.38	2.05	1.78	.548	.120	.025
75	9.75	6.23	5.09	4.17	3.45	2.87	2.41	2.04	1.74	1.49	.420	.088	.018
85	9.63	5.91	4.72	3.80	3.08	2.53	2.09	1.75	1.47	1.25	.329	.070	.014
95	9.51	5.39	4.26	3.39	2.73	2.22	1.82	1.50	1.25	1.05	.263	.052	.011
999	7.20	.369	.137	.064	.036	.022	.015	.011	.008	.007	.001	0	0

Table 2. Values of $\frac{\rho Z_o H_\phi}{V_o} \times 10^3$

$T_\theta \backslash \beta_\theta$	1	2	4	6	8	10	20	40	60	80	10^2	10^3	10^4
.2	179	108	62.3	44.1	35.2	29.1	16.3	7.23	4.46	3.34	2.67	.267	.027
.4	132	80.2	45.1	32.8	24.9	20.2	11.2	5.00	3.28	2.47	1.97	.197	.020
.8	105	63.8	36.2	26.1	19.2	15.8	8.82	4.62	2.70	2.03	1.62	.162	.016
1.4	103	64.5	36.7	25.6	19.7	16.0	8.26	4.24	2.87	2.17	1.74	.174	.017
1.9	183	123	73.1	51.8	40.0	32.6	16.9	8.59	5.76	4.33	3.62	.362	.036
3.0	17.4	6.24	2.03	1.03	.630	.430	.130	.038	.019	.011	.007	0	0
4.1	62.0	25.2	8.36	4.11	2.44	1.61	.430	.112	.050	.028	.018		
5.0	19.0	7.03	2.22	1.07	.628	.412	.109	.028	.013	.007	.005		
5.9	2.44	1.76	.835	.464	.292	.200	.057	.015	.007	.004	.003		
7.0	14.2	4.21	1.08	.478	.266	.169	.041	.010	.005	.003	.002		
8.1	5.51	2.22	.673	.310	.176	.113	.028	.007	.003	.002	.001		
9.0	8.39	2.32	.580	.253	.140	.089	.022	.005	.002	.001	.001		
9.9	8.31	2.02	.474	.204	.112	.071	.017	.004	.002	.001	.001		
13	4.23	1.07	.252	.108	.060	.038	.009	.002	.001	.001	0		
17	2.58	.603	.139	.060	.033	.021	.005	.001	.001	0			
23	1.40	.314	.072	.031	.017	.011	.003	.001	0				
29	.860	.190	.044	.019	.010	.007	.002	0					
35	.576	.127	.029	.013	.007	.004	.001						
45	.334	.074	.017	.008	.004	.003	.001						
55	.216	.048	.011	.005	.003	.002	0						
65	.151	.034	.008	.004	.002	.001							
75	.111	.025	.006	.003	.001	.001							
85	.084	.019	.005	.002	.001	.001							
95	.067	.015	.004	.002	.001	.001							
999	0	0	0	0	0	0							

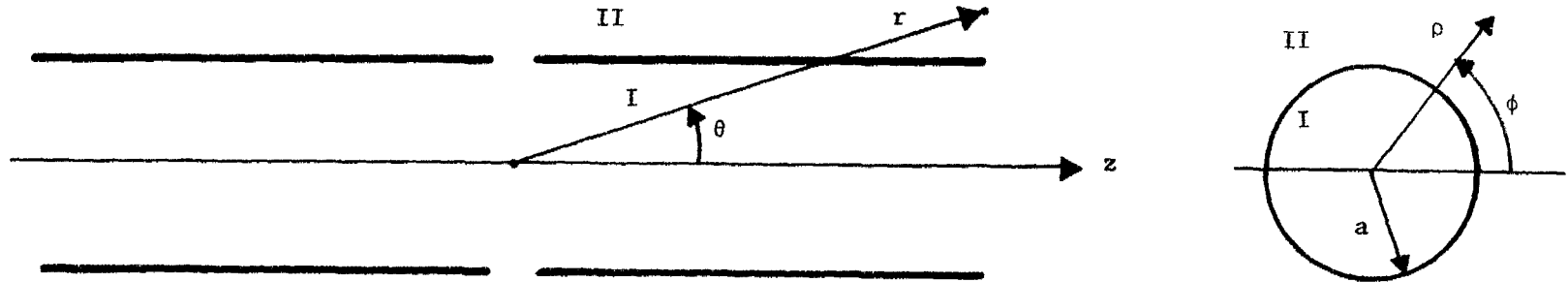


Figure 1. The geometry of the problem.

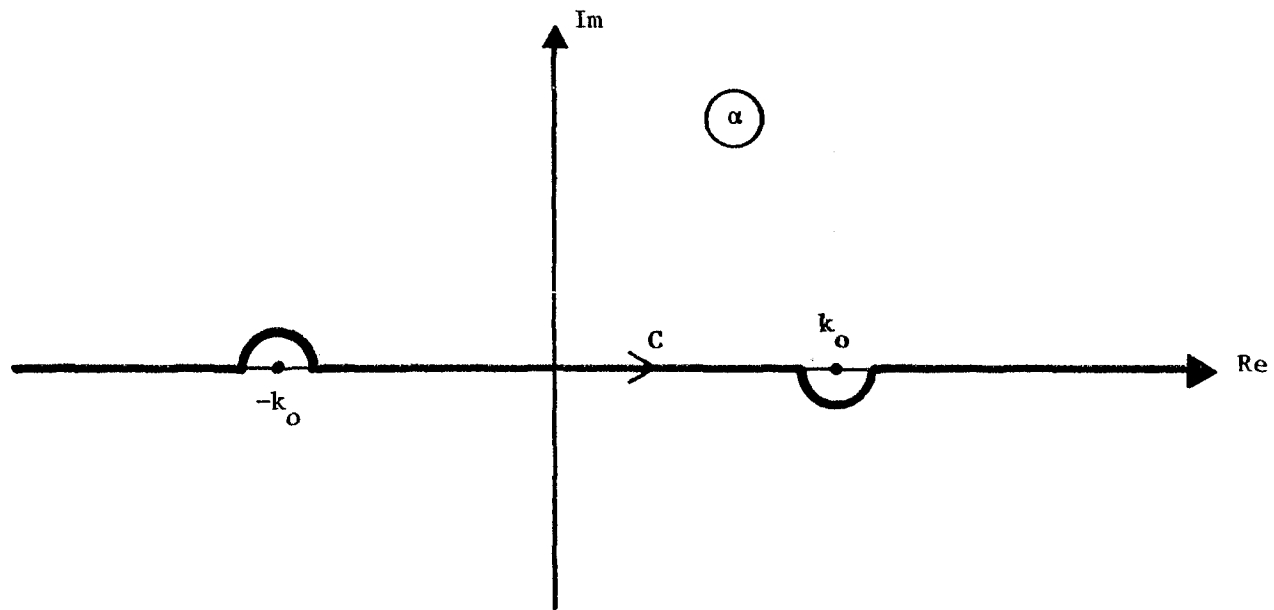


Figure 2. The path of integration for the inverse Fourier transform.

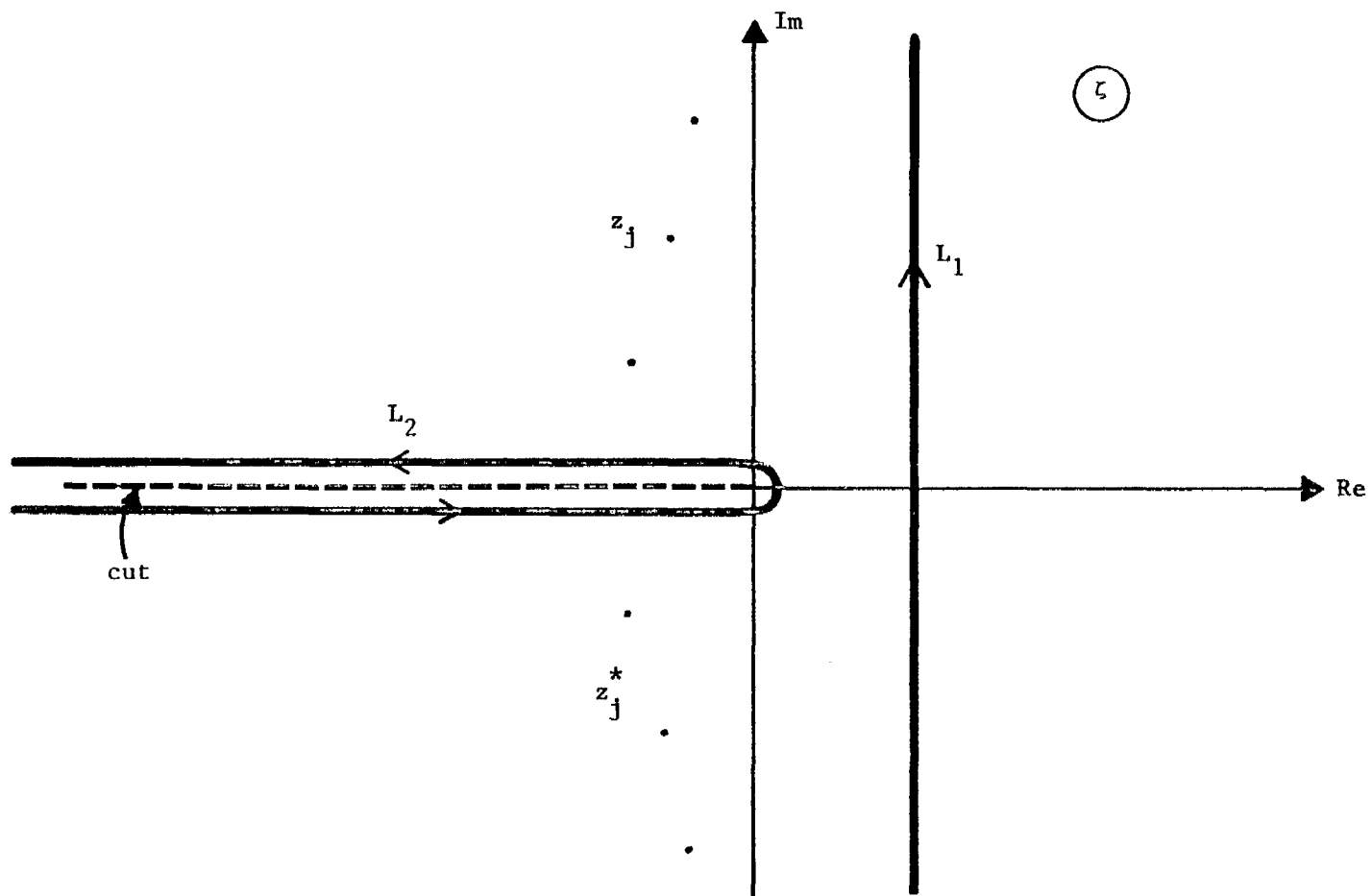


Figure 3. The path of integration for the inverse Laplace transform.

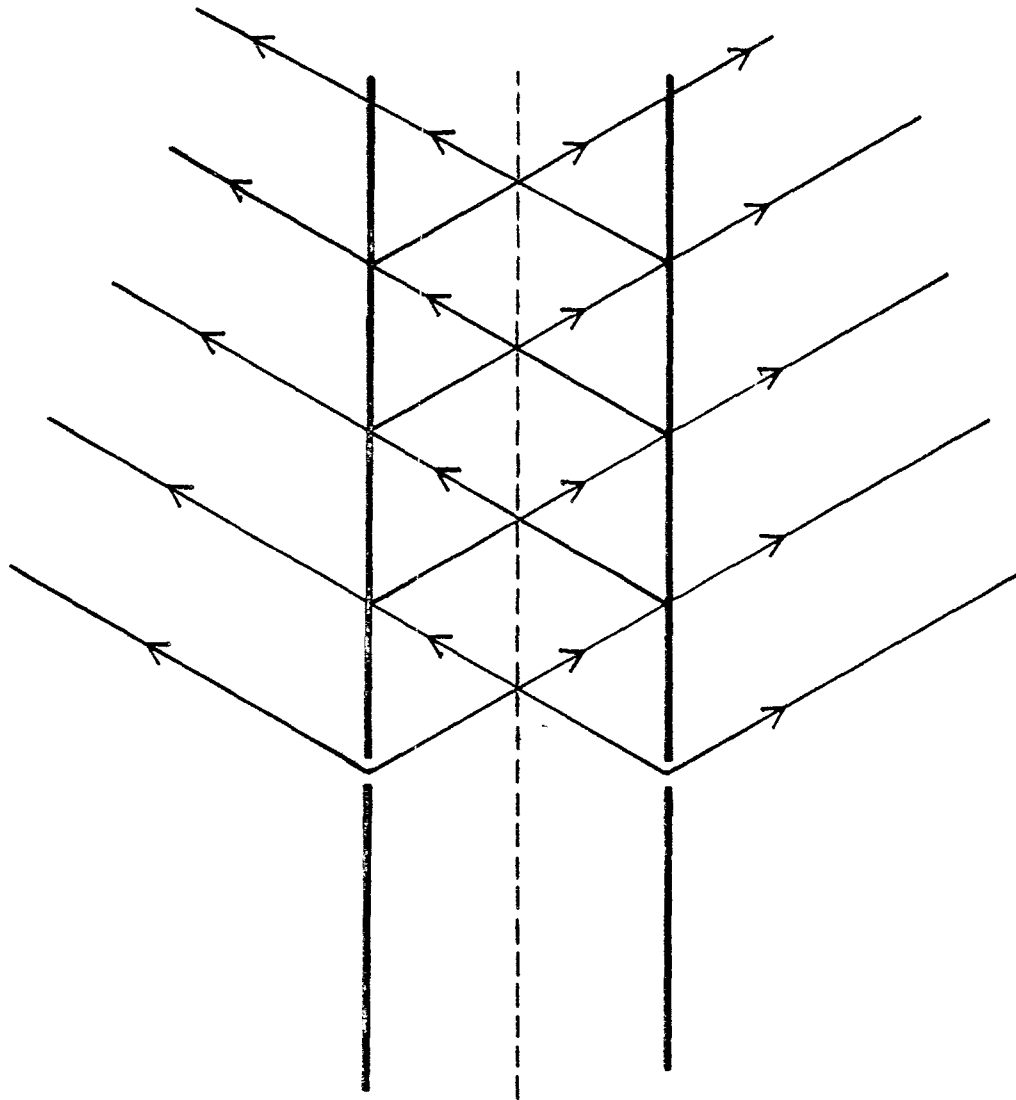


Figure 4. Reflection and transmission of the wave fronts.

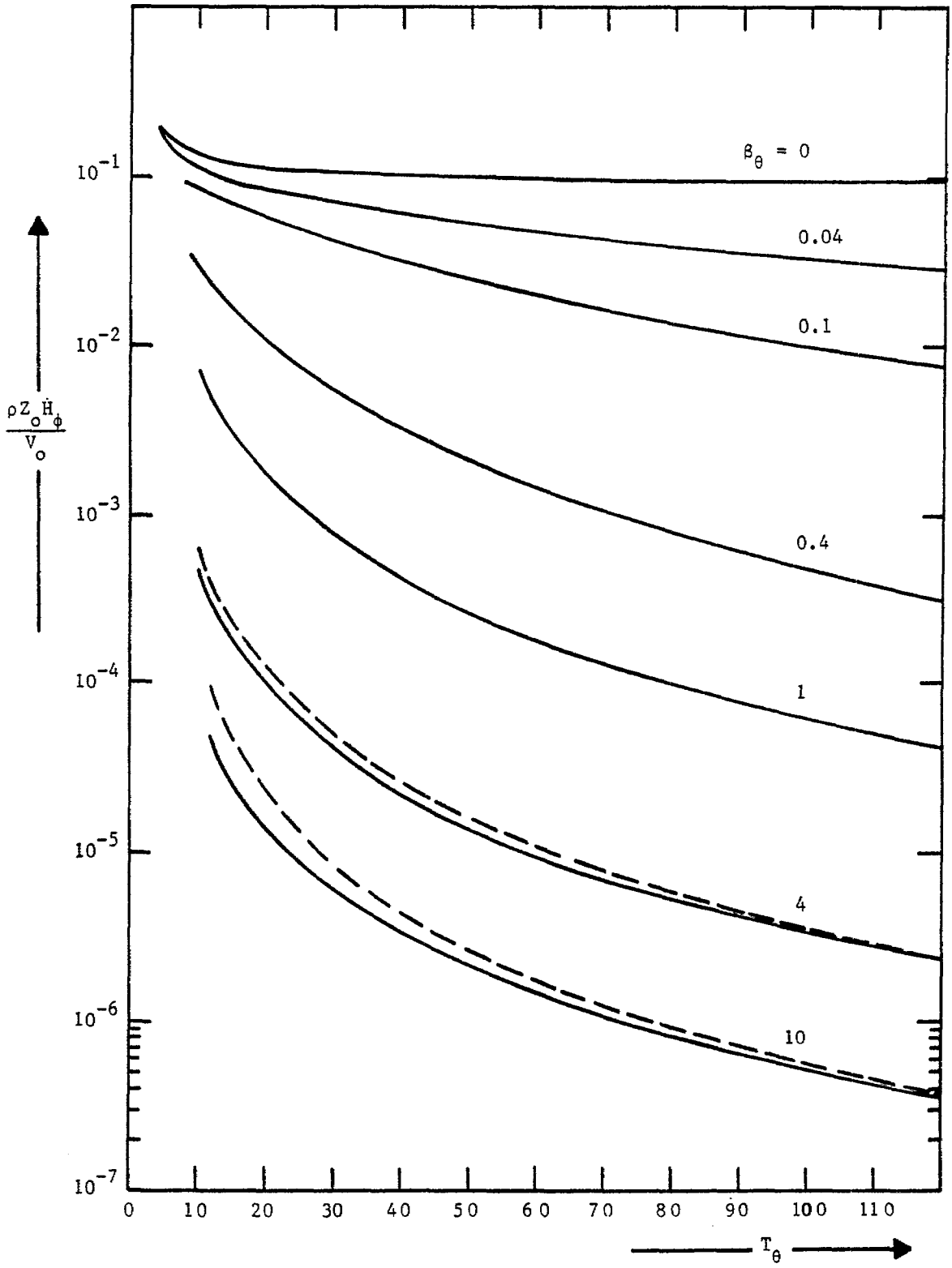


Figure 5. Radiation field for a step-function voltage.
The singularities at $T_\theta = 2n$ have been omitted.

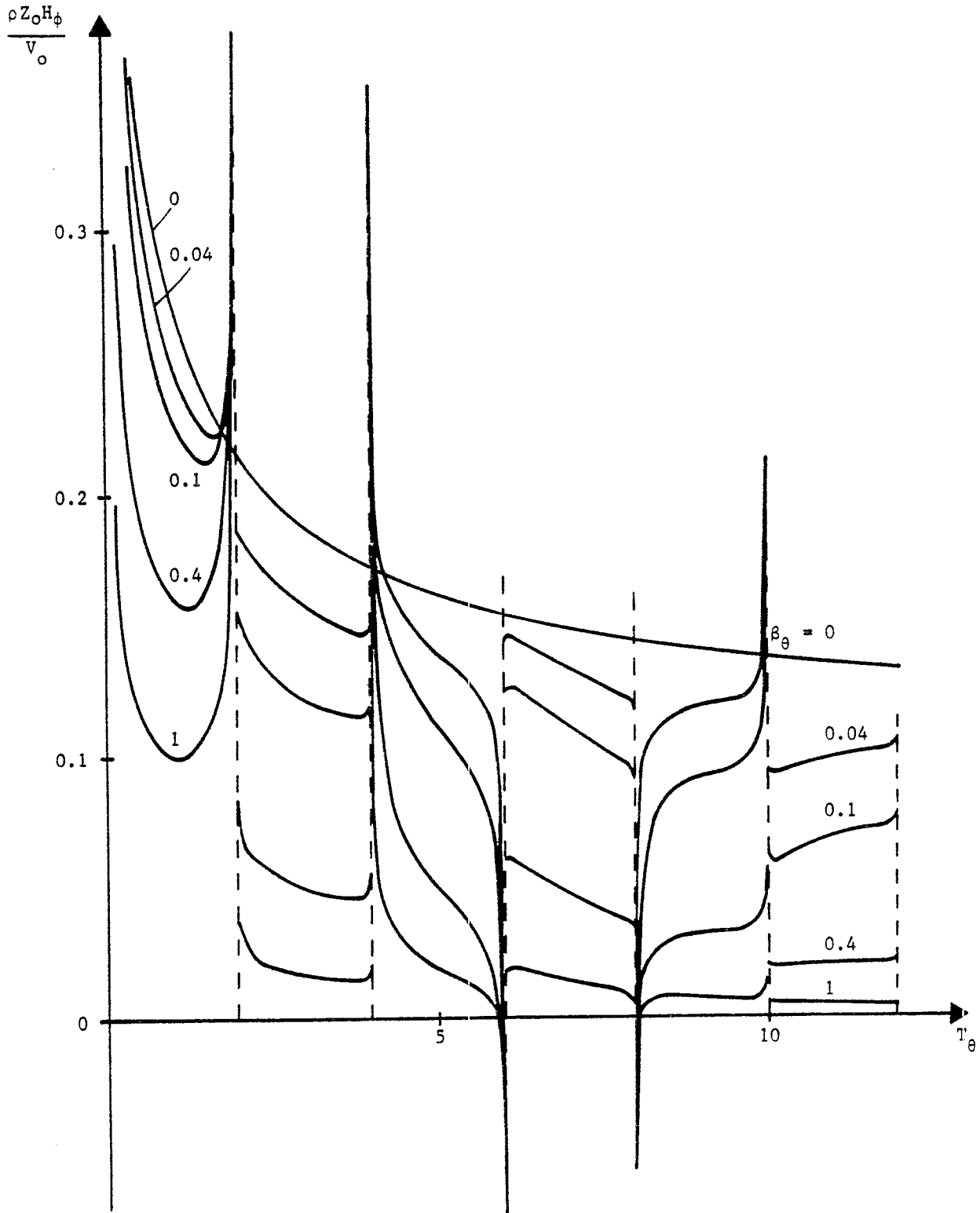


Figure 6. Radiation field for a step-function voltage.

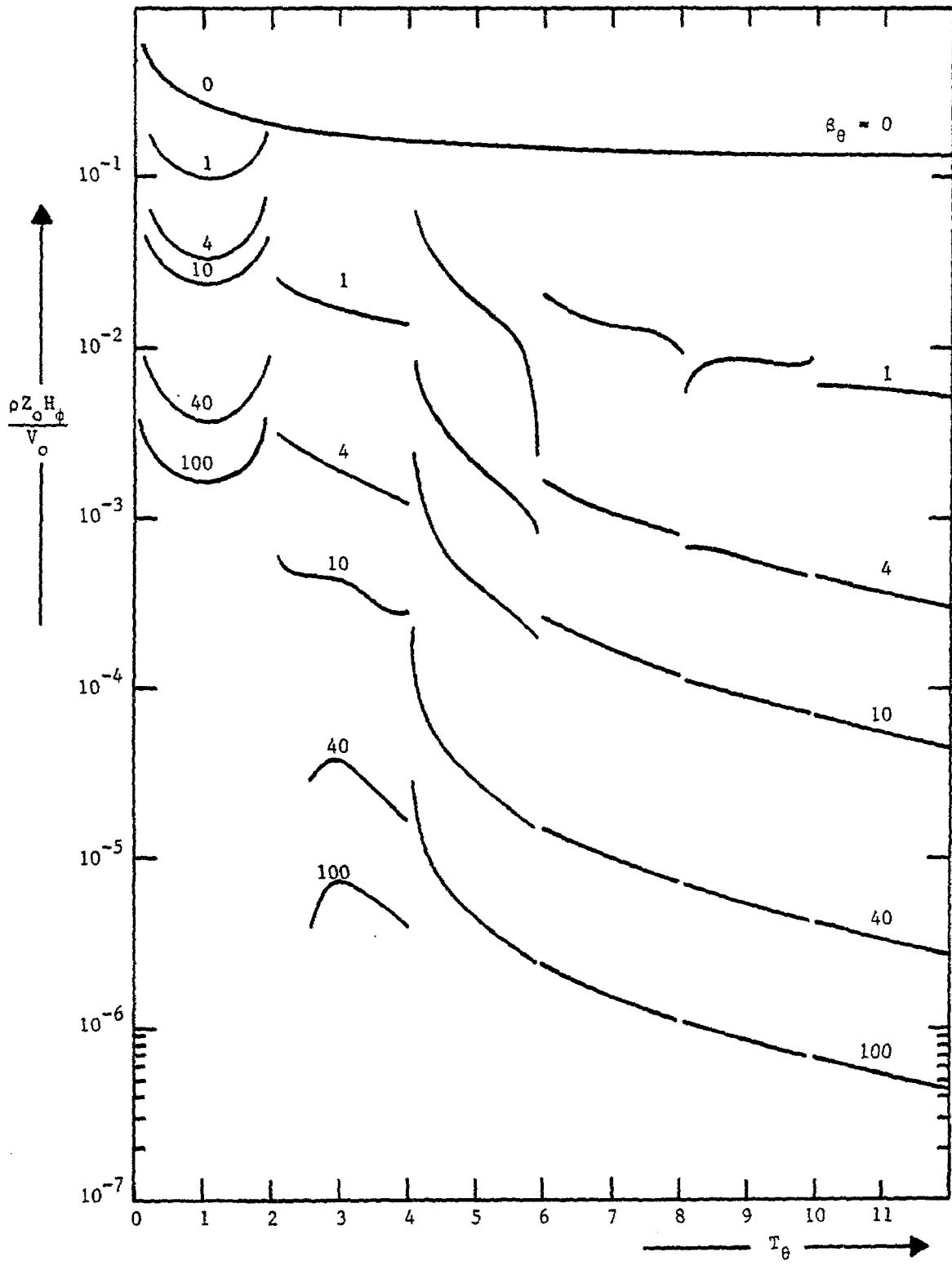


Figure 7. Radiation field for a step-function voltage.

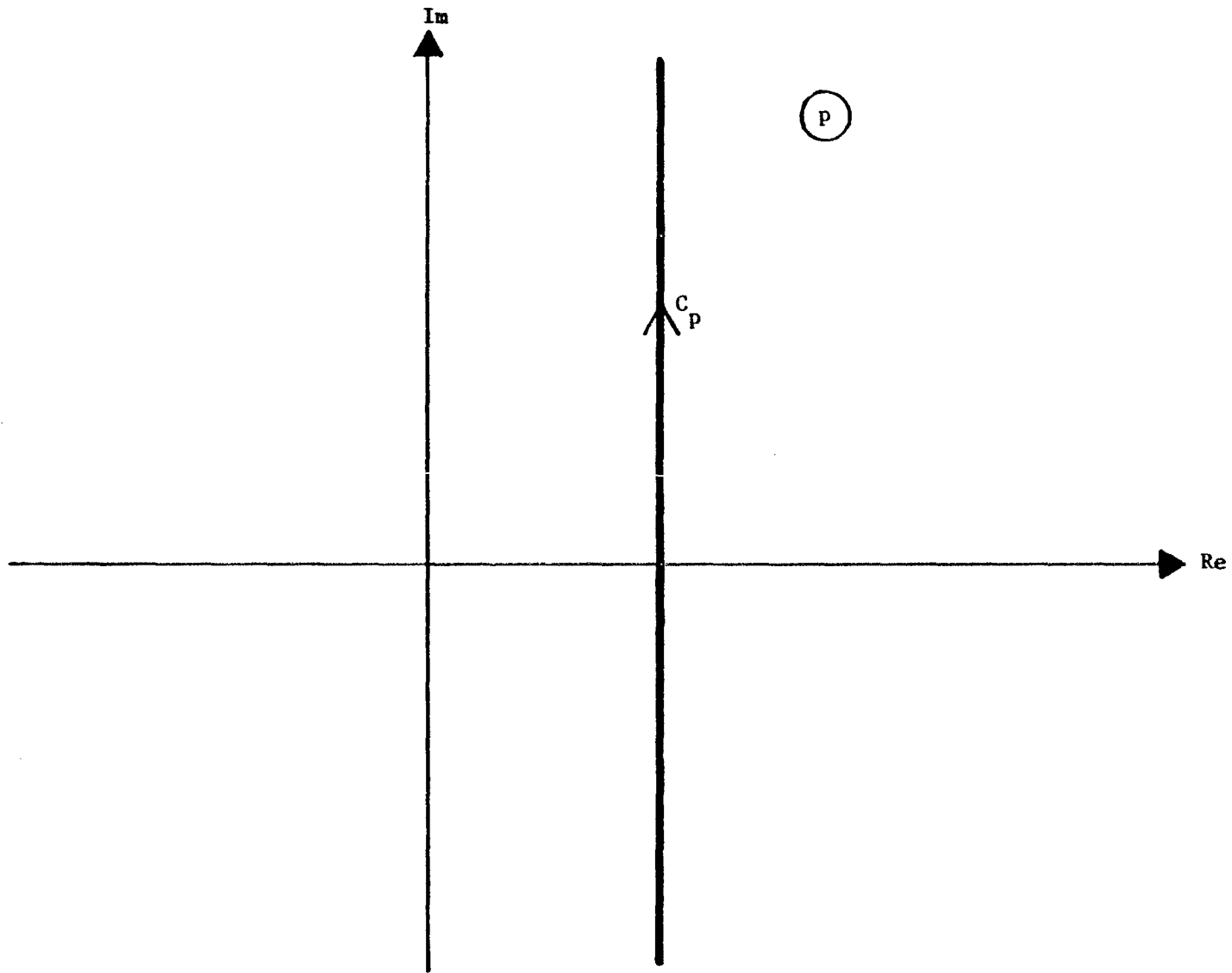


Figure 8. The path of integration for the inverse Laplace transform.

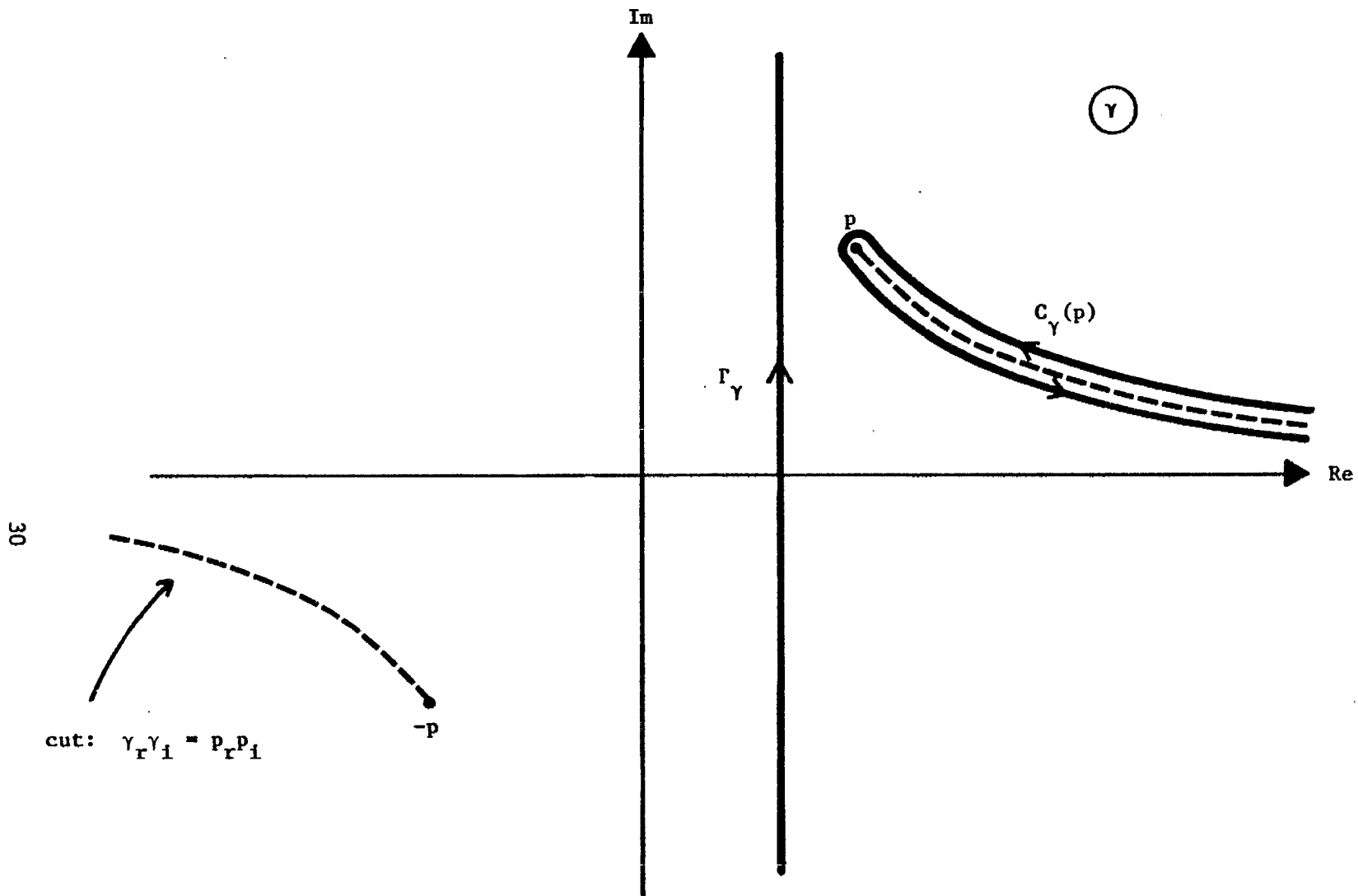


Figure 9. Paths of integration on the branch of $\alpha = \sqrt{\gamma^2 - p^2}$ where $\alpha = ip$ at $\gamma = 0$.

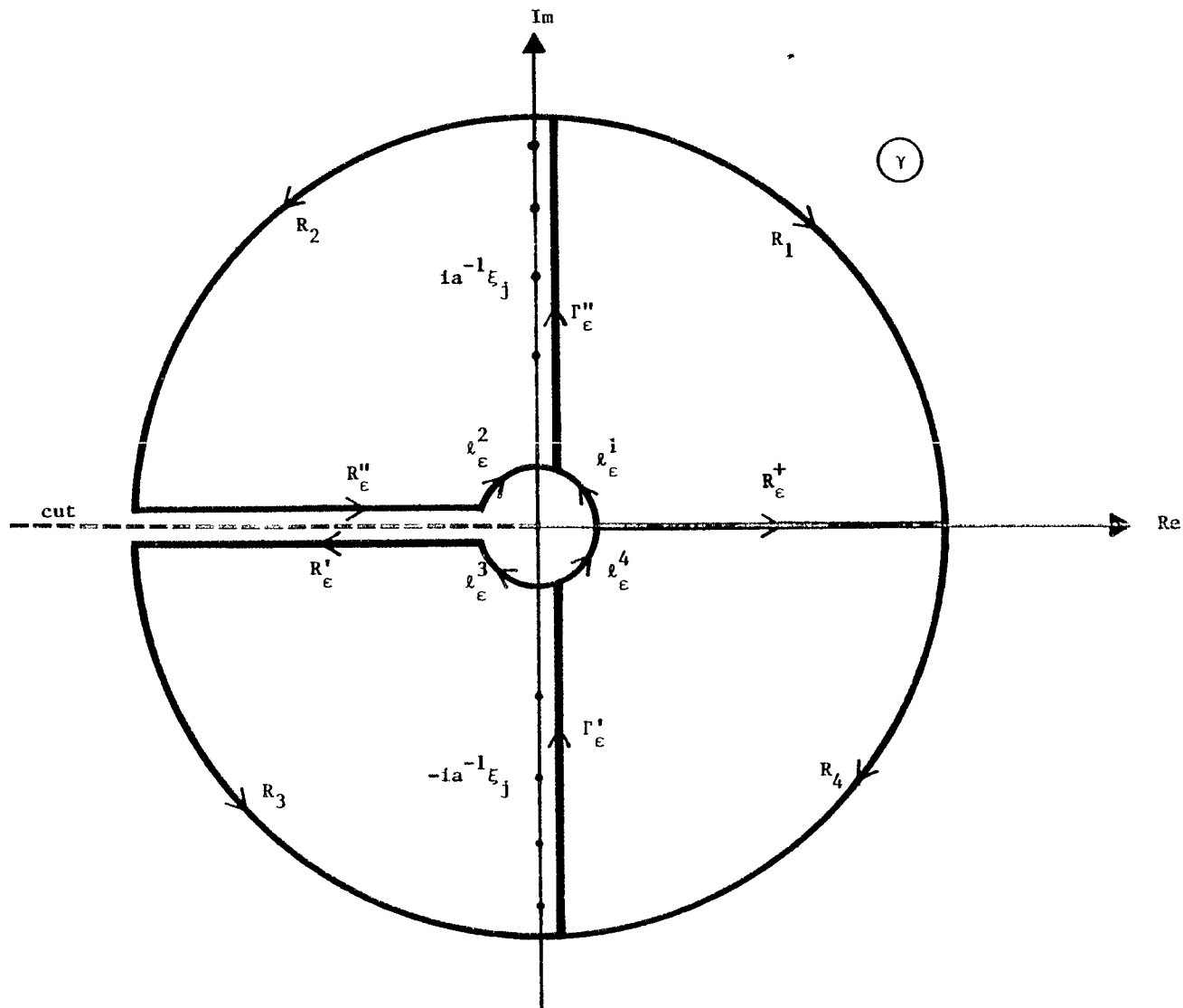


Figure 10. Paths of integration on the branch where $|\arg\{\gamma\}| < \pi$.

Appendix A

In this appendix we are going to show that for $\text{Re}\{\beta\} > 0$, $g(z) = \beta + zI_0(z)K_0(z)$, has no zeros for $|\arg\{z\}| \leq \pi/2$.

The function $g(z)$ is analytic in the z -plane except for the branch-cut from the origin to infinity along the real negative axis. We will calculate the number of zeros (N) of g in the right half plane by calculating the change of the argument of g along the contour L :

$$L = L^- + L^+ \quad (A1)$$

where L^- and L^+ are respectively the unions of L_j^- and L_j^+ , $j = 1, 2, 3, 4$. L_j^\pm are pointed out in figure 11 and will be described below. Then we will let "L tend to infinity".

At P we have: $\arg\{g(P)\} = \arg\{\beta\} = \theta_0$, $-\pi/2 < \theta_0 < \pi/2$. Let L_1^- be a curve with equation: $|z| = \delta$, $-\pi/2 \leq \arg\{z\} \leq 0$. When $\delta \rightarrow 0$ we have: $g(z) \sim \beta$, $z \in L_1^-$ and thus $\arg\{g(R^-)\} = \theta_0$.

Let L_2^- be a line with equation: $z = y \exp(-i\pi/2)$, $0 < y \leq y_0$. Then on L_2^- : $g(z) = \beta + 0.5\pi y J_0^2(y) + 0.5i\pi y J_0(y)Y_0(y)$. With S^- the point $y_0 \exp(-i\pi/2)$ and as $\text{Re}\{\beta\} > 0$ we have: $\arg\{g(S^-)\} = \theta_1(y_0)$, $-\pi/2 < \theta_1(y_0) < \pi/2$.

Let Q^- be the point $x_0 + y_0 \exp(-i\pi/2)$ and L_3^- the line $z = x + y_0 \exp(-i\pi/2)$ $0 \leq x \leq x_0$. Suppose also that y_0 is such that on L_3^- we can use asymptotic expressions for the Bessel functions involved. Then on L_3^- : $g(z) \sim \beta + 0.5 + 0.5 \exp(-2x + i2y_0)$, and thus $\arg\{g(Q^-)\} = \theta_2 + \theta_3(x_0, y_0)$. Here $\theta_2 = \arg\{\beta + 0.5\}$, $-\pi/2 < \theta_2 < \pi/2$ and

$$\lim_{(x_0, y_0) \rightarrow (\infty, \infty)} \theta_3(x_0, y_0) = 0.$$

Let L_4^- be the line $z = x_0 + y \exp(-i\pi/2)$, $0 \leq y \leq y_0$, and let x_0 be such that on L_4^- we have $g(z) \sim \beta + 0.5 \exp(-2x_0 + 2iy)$. Thus with T the point x_0 : $\arg\{g(T)\} = \theta_2 + \theta_4(x_0)$ and $\lim_{x_0 \rightarrow \infty} \theta_4(x_0) = 0$.

Thus

$$\lim_{(x_0, y_0) \rightarrow (\infty, \infty)} \Delta_- \arg\{g(z)\} = \theta_2 - \theta_0. \quad (A2)$$

In the same way we have

$$\lim_{(x_0, y_0) \rightarrow (\infty, \infty)} \Delta_+ \arg\{g(z)\} = -\theta_2 + \theta_0. \quad (A3)$$

Finally

$$N = (2\pi)^{-1} [\Delta_+ \arg\{g(z)\} + \Delta_- \arg\{g(z)\}] = 0 \quad (A4)$$

which means that $g(z)$ has no zeros in the right half plane.

Appendix B

We will here deduce an asymptotic expression for the zeros, z_j , of $g(z) = \beta + zI_0(z)K_0(z)$ valid when $|z_j| \gg 1$.

Using the asymptotic expression for $I_0(z)$, $K_0(z)$ valid when $|z| \gg 1$, $0 \leq \arg\{z\} \leq \pi$ we have

$$2g(z) \sim 2\beta + 1 + \frac{1}{8z^2} + i\left(1 - \frac{1}{4z} + \frac{5}{32z^2} - \frac{21}{128z^3}\right)e^{-2z}. \quad (B1)$$

As a first approximation of the zeros, z_j , fulfilling $|z_j| \gg 1$, $0 \leq \arg\{z_j\} \leq \pi$ we use z_j' where z_j' satisfies

$$2\beta + 1 + ie^{-2z_j'} = 0$$

and

$$z_j' = z_r + i\tau_j \quad (B2)$$

where $z_r = -0.5 \ln(1 + 2\beta)$ and $\tau_j = j\pi - \pi/4$, j integer ≥ 1 . We assume that $\tau_j \gg |z_r|$, $\tau_j \gg 1$. Next we make the expansion

$$z_j \approx i\tau_j + z_r + ia\tau_j^{-1} + b\tau_j^{-2} + ic\tau_j^{-3} \quad (B3)$$

and we assume $|a\tau_j^{-1}| \ll 1$, $|b\tau_j^{-2}| \ll 1$, $|c\tau_j^{-3}| \ll 1$. Expanding (B1) in a power series with respect to τ_j^{-1} and putting the coefficients for $\tau_j^{-\mu}$ ($\mu = 1, 2, 3$) equal to zero we get

$$a = 0.125$$

$$b = \frac{1}{16(1+2\beta)} - \frac{z_r}{8} - \frac{1}{16} \quad (B4)$$

$$c = -\frac{31}{384} + \frac{8z_r + 2\beta}{32(1+2\beta)} - \frac{3z_r}{16} - \frac{z_r^2}{4}$$

For $\beta \ll 1$ we have $z_r \approx -\beta - \beta^2$, $b \approx 0.125\beta^2$, $c \approx -31/384 - \beta^2/8$.

For the zeros, z_j , $|z_j| \gg 1$, $-\pi \leq \arg\{z_j\} \leq 0$ we use the asymptotic expression for $g(z)$ valid when $-\pi \leq \arg\{z\} \leq 0$

$$2g(z) \sim 2\beta + 1 + \frac{1}{8z^2} - i\left(1 - \frac{1}{4z} + \frac{5}{32z^2} - \frac{21}{128z^3}\right)e^{-2z} \quad (B5)$$

In this case we have the following asymptotic expression for z_j :

$$z_j \approx -i\tau_j + z_r - ia\tau_j^{-1} + b\tau_j^{-2} - ic\tau_j^{-3} \quad (B6)$$

where τ_j , z_r , a , b , c are given by (B2) and (B4). Note that

$$1^\circ \operatorname{Re}\{z_j\} < 0, \operatorname{Re}\{\beta\} > 0$$

$$2^\circ \lim_{\beta \rightarrow 0} z_j = \pm i\left(\tau_j + \frac{1}{8\tau_j} - \frac{31}{384\tau_j^3}\right)$$

and this expression coincides with the asymptotic expression for the zeros of $I_0(z)$ (c.f.⁶ p. 505).

Appendix C

In this appendix we will derive a method for numerical calculation of $S(T_\theta, \beta_\theta)$ defined by (17) in section III.

$$0 < T_\theta < 20$$

Introduce

$$S'(T_\theta, \beta_\theta, N) = \sum_{j=N}^{\infty} \frac{I_0(z_j) e^{(T_\theta-1)z_j}}{g'(z_j, \beta_\theta)} \quad (C1)$$

and

$$S(T_\theta, \beta_\theta) = \text{Re}\{S'(T_\theta, \beta_\theta, 21)\} \quad (C2)$$

But for $|z_j|$ large we have

$$\frac{I_0(z_j) e^{-i\tau_j - z_r}}{g'(z_j, \beta_\theta)} \sim \frac{i\sqrt{i}}{\sqrt{2\pi}} \cdot \frac{2\beta_\theta}{1 + 2\beta_\theta} \left\{ \frac{1}{\sqrt{\tau_j}} + \frac{iz_r}{2\tau_j \sqrt{\tau_j}} \right\}$$

and

$$e^{i\tau_j + z_r} e^{(T_\theta-1)z_j} \sim$$

$$e^{i\tau_j T_\theta} e^{T_\theta z_r} \left\{ 1 + \frac{i(T_\theta-1)}{8\tau_j} + \frac{b(T_\theta-1)}{\tau_j^2} - \frac{(T_\theta-1)^2}{132\tau_j^2} + \frac{ic(T_\theta-1)}{\tau_j^3} - \frac{i(T_\theta-1)^3}{3072\tau_j^3} \right\}$$

Thus,

$$\begin{aligned}
S'(T_\theta, \beta_\theta, N) &\approx \frac{i\sqrt{i}\sqrt{2}\beta_\theta e^{T_\theta z_r}}{\sqrt{\pi}(1+2\beta_\theta)} \{S_0(T_\theta, N) \\
&+ \frac{i(4z_r + T_\theta - 1)}{8} S_1(T_\theta, N) + [(b - \frac{z_r}{16})(T_\theta - 1) - \frac{(T_\theta - 1)^2}{132}] S_2(T_\theta, N) \\
&+ i[(c + 0.5z_r b)(T_\theta - 1) - \frac{z_r(T_\theta - 1)^2}{264} - \frac{(T_\theta - 1)^3}{3072}] S_3(T_\theta, N)\} \quad (C3)
\end{aligned}$$

where

$$S_m(T_\theta, N) = \sum_{j=N}^{\infty} \frac{e^{i\tau_j T_\theta}}{\tau_j^{m+0.5}}, \quad m = 0, 1, 2, 3$$

But

$$\frac{e^{i\tau u}}{\tau^{m+0.5}} = \frac{e^{i\tau u}}{(m-0.5)!} \int_0^{\infty} x^{m-0.5} e^{-\tau x} dx$$

and from the proof given in appendix D it follows

$$S_m(T_\theta, N) = \frac{e^{i\tau_N T_\theta}}{(m-0.5)!} \int_0^{\infty} \frac{x^{m-0.5} e^{-\tau_N x}}{1 - e^{-i\pi T_\theta} e^{-\pi x}} dx$$

Note that $S_0(T_\theta, N)$ has singularities at $T_\theta = 2n$, n nonnegative integer. An investigation of the behavior of $S_0(T_\theta, N)$ around the singularities is given in appendix E.

Finally we get for $S(T_\theta, \beta_\theta)$

$$\begin{aligned}
S(T_\theta, \beta_\theta) \approx & \frac{\sqrt{2\beta_\theta}}{\pi(1+2\beta_\theta)} \frac{1}{1+0.5T_\theta} \left\{ \sin(\tau_{20}T_\theta + \frac{\pi}{4})L_0(\tau_{22}, T_\theta) - \sin(\tau_{21}T_\theta + \frac{\pi}{4})L_0(\tau_{21}, T_\theta) \right. \\
& + \frac{4z_r + T_\theta - 1}{8} \left[\sin(\tau_{21}T_\theta - \frac{\pi}{4})L_1(\tau_{21}, T_\theta) - \sin(\tau_{20}T_\theta - \frac{\pi}{4})L_1(\tau_{22}, T_\theta) \right] \\
& + \left[(b - \frac{z_r}{16})(T_\theta - 1) - \frac{(T_\theta - 1)^2}{132} \right] \times \left[\sin(\tau_{20}T_\theta + \frac{\pi}{4})L_2(\tau_{22}, T_\theta) \right. \\
& - \left. \sin(\tau_{21}T_\theta + \frac{\pi}{4})L_2(\tau_{21}, T_\theta) \right] + \left[(c + \frac{z_r b}{2})(T_\theta - 1) - \frac{z_r(T_\theta - 1)^2}{264} - \frac{(T_\theta - 1)^3}{3072} \right] \\
& \times \left[\sin(\tau_{21}T_\theta - \frac{\pi}{4})L_3(\tau_{21}, T_\theta) - \sin(\tau_{20}T_\theta - \frac{\pi}{4})L_3(\tau_{22}, T_\theta) \right] \quad (C4)
\end{aligned}$$

where

$$L_m(s, T_\theta) = \ell_m \int_0^\infty \frac{x^{m-0.5} e^{-sx}}{1 + e^{-2\pi x} - 2e^{-\pi x} \cos(\pi T_\theta)} dx$$

and

$$\ell_m = \frac{\sqrt{\pi}}{(m-0.5)!} = \begin{cases} 1, & m = 0 \\ \frac{2^m}{(2m-1)!!}, & m \geq 1 \end{cases}$$

We estimate the error of $S(T_\theta, \beta_\theta)$ by estimating the magnitude of the last term in $S'(T_\theta, \beta_\theta, 21)$. Introduce

$$\Delta_N = [(c+0.5z_r b)(T_\theta - 1) - \frac{z_r (T_\theta - 1)^2}{264} - \frac{(T_\theta - 1)^3}{3072}] s_3(T_\theta, N)$$

$$|\Delta_N| < \frac{|c+0.5z_r b| |T_\theta - 1| + \frac{|z_r| (T_\theta - 1)^2}{264} + \frac{|T_\theta - 1|^3}{3072}}{\sqrt{2\pi} (2.5)! (\tau_N)^{3.5} (1+2\beta_\theta)^{0.5T_\theta}} \int_0^\infty \frac{x^{2.5} e^{-x}}{|1 - e^{\frac{i\pi T_\theta \tau_N^{-1} - \pi x \tau_N^{-1}}{e}}|} dx$$

But

$$\int_0^\infty \frac{x^{2.5} e^{-x}}{|1 - e^{\frac{i\pi T_\theta \tau_N^{-1} - \pi x \tau_N^{-1}}{e}}|} dx \leq (N - \frac{1}{4})(1.5)!$$

and $\frac{|z_r| (T_\theta - 1)^2}{264 (1+2\beta_\theta)^{0.5T_\theta}} < 0.3$ and $\frac{|T_\theta - 1|^3}{3072 (1+2\beta_\theta)^{0.5T_\theta}} < 2.2$ for $T_\theta \leq 20$. Moreover

$$\max_{T_\theta} \left\{ \frac{T_\theta - 1}{(1+2\beta_\theta)^{0.5T_\theta}} \right\} = \frac{2}{e\sqrt{1+2\beta_\theta}} \text{ for } T_\theta = 1 + \frac{2}{\ln(1+2\beta_\theta)}$$

and thus,

$$\frac{|2c+z_r b| |T_\theta - 1|}{2(1+2\beta_\theta)^{0.5T_\theta}} \leq \frac{|2c+z_r b|}{e\sqrt{1+2\beta_\theta}}$$

Finally

$$\frac{|2c+z_r b|}{e\sqrt{1+2\beta_\theta}} \leq \frac{1}{e} \max_{\beta_\theta} \frac{2|c| + |z_r b|}{\sqrt{1+2\beta_\theta}} < 2.3$$

From this we get $|\Delta_{21}| < 10^{-5}$.

$$\underline{T_\theta > 20}$$

Put

$$S'(T_\theta, \beta_\theta, N) = Q'(T_\theta, \beta_\theta, N) + U'(T_\theta, \beta_\theta)$$

where

$$Q'(T_\theta, \beta_\theta, N) = \sum_{j=N}^{[T_\theta]} \frac{I_0(z_j) e^{(T_\theta-1)z_j}}{g'(z_j, \beta_\theta)}$$

$$U'(T_\theta, \beta_\theta) = \sum_{[T_\theta]+1}^{\infty} \frac{I_0(z_j) e^{(T_\theta-1)z_j}}{g'(z_j, \beta_\theta)}$$

and

$$Q'(T_\theta, \beta_\theta, N) \approx \frac{i\sqrt{2i/\pi} \beta_\theta e^{z_r T_\theta}}{1 + 2\beta_\theta} \sum_{j=N}^{[T_\theta]} \frac{1}{\sqrt{\tau_j}} \left(1 + \frac{iz_r}{2\tau_j}\right) e^{i\tau_j T_\theta} \delta_j T_\theta$$

where $\delta_j = 0.125i\tau_j^{-1} + b\tau_j^{-2} + ic\tau_j^{-3}$. Moreover

$$U'(T_\theta, \beta_\theta) \approx \frac{i\sqrt{2i/\pi} \beta_\theta e^{T_\theta z_r}}{1 + 2\beta_\theta} \left\{ S_0(T_\theta, N_\theta) + \frac{i(4z_r + T_\theta - 1)}{8} S_1(T_\theta, N_\theta) \right.$$

$$\left. + \left[\left(b - \frac{z_r}{16}\right) (T_\theta - 1) - \frac{(T_\theta - 1)^2}{132} \right] S_2(T_\theta, N_\theta) \right.$$

$$\left. + i \left[\left(c + \frac{z_r b}{2}\right) (T_\theta - 1) - \frac{z_r (T_\theta - 1)^2}{264} - \frac{(T_\theta - 1)^3}{3072} \right] S_3(T_\theta, N_\theta) \right\}$$

where

$$N_{\theta} = [T_{\theta}] + 1, \quad T_{\theta} < N_{\theta} \leq T_{\theta} + 1$$

From this we get:

$$\begin{aligned}
 S(T_{\theta}, \beta_{\theta}) \approx & \frac{\sqrt{2} \beta_{\theta}}{\pi(1+2\beta_{\theta})} \frac{1+0.5T_{\theta}}{\sum_{j=21}^{[T_{\theta}]} \frac{\sin[(\tau_j + \Delta_j)T_{\theta} + \pi/4] e^{bT_{\theta}\tau_j^{-2}}}{\sqrt{\tau_j}}} \\
 & + \sum_{j=21}^{[T_{\theta}]} 0.5\tau_j^{-3/2} z_r \frac{\sin[(\tau_j + \Delta_j)T_{\theta} - \pi/4] e^{bT_{\theta}\tau_j^{-2}}}{\sqrt{\tau_j}} \\
 & + \sin(\tau_{M_{\theta}} T_{\theta} + \pi/4) L_0(\tau_{P_{\theta}}, T_{\theta}) - \sin(\tau_{N_{\theta}} T_{\theta} + \pi/4) L_0(\tau_{N_{\theta}}, T_{\theta}) \\
 & + \frac{4z_r T_{\theta} - 1}{8} [\sin(\tau_{N_{\theta}} T_{\theta} - \pi/4) L_1(\tau_{N_{\theta}}, T_{\theta}) - \sin(\tau_{M_{\theta}} T_{\theta} - \pi/4) L_1(\tau_{P_{\theta}}, T_{\theta})] \\
 & + [(b - z_r/16)(T_{\theta} - 1) - \frac{(T_{\theta} - 1)^2}{132}] \times [\sin(\tau_{M_{\theta}} T_{\theta} + \pi/4) L_2(\tau_{P_{\theta}}, T_{\theta}) \\
 & - \sin(\tau_{N_{\theta}} T_{\theta} + \pi/4) L_2(\tau_{N_{\theta}}, T_{\theta})] + [(c + z_r b/2)(T_{\theta} - 1) - \frac{z_r(T_{\theta} - 1)^2}{264} - \frac{(T_{\theta} - 1)^3}{3072}] \\
 & \times [\sin(\tau_{N_{\theta}} T_{\theta} - \pi/4) L_3(\tau_{N_{\theta}}, T_{\theta}) - \sin(\tau_{M_{\theta}} T_{\theta} - \pi/4) L_3(\tau_{P_{\theta}}, T_{\theta})] \quad (C6)
 \end{aligned}$$

where $\Delta_j = 0.125\tau_j^{-1} + c\tau_j^{-3}$, $M_\theta = N_\theta - 1$, $P_\theta = N_\theta + 1$.

In order to get an estimate of the error, Δ_S , of $S(T_\theta, \beta_\theta)$ we use:

$|\Delta_S| = |\Delta_Q| + |\Delta_U|$ where Δ_Q is an estimate of the error of $Q'(T_\theta, \beta_\theta, 21)$ and Δ_U an estimate of the error of $U'(T_\theta, \beta_\theta)$. Let δ' be the maximum error of δ_j . Then

$$|\Delta_Q| < \frac{\sqrt{2}\delta T_\theta \beta_\theta}{(1+2\beta_\theta)} \left[\frac{1+0.5T_\theta}{\sqrt{T_\theta}} - \sqrt{20} - \frac{|z_r|}{2\pi\sqrt{T_\theta}} + \frac{|z_r|}{2\pi\sqrt{20}} \right]$$

As an estimate of δ we use $\delta = \tau_{21}^{-3}|c|$ and one can show that

$$|\Delta_Q| < 0.9\tau_{21}^{-3} < 4 \times 10^{-6}.$$

Proceeding as on page 39 we have for Δ_U

$$|\Delta_U| < \frac{\beta_\theta (|2c+z_r b| |T_\theta - 1| + \frac{|z_r| (T_\theta - 1)^2}{132} + \frac{|T_\theta - 1|^3}{1536})}{350 |T_\theta - 1|^{2.5} (1+2\beta_\theta)^{1+0.5T_\theta}}$$

and $|\Delta_U| < 5 \times 10^{-6}$. Thus, $|\Delta_S| < 10^{-5}$.

Before concluding this appendix we wish to estimate the error Δ_A of $A(T_\theta, \beta_\theta)$. Let δ' be the error of z_j , then

$$|\Delta_A| \sim \frac{40\delta' T_\theta \beta_\theta}{\sqrt{2\pi} (1+2\beta_\theta)^{1+0.5T_\theta}}$$

and $|\Delta_A| < 6\delta'$. When $\delta' = 10^{-6}$, $|\Delta_A| < 6 \times 10^{-6}$.

Appendix D

In this appendix we will prove that

$$S_m(u, N) = \sum_{j=N}^{\infty} \frac{e^{i\tau_j u}}{\tau_j^{m+0.5}} = \frac{e^{i\tau_N u}}{(m-0.5)!} \int_0^{\infty} \frac{x^{m-0.5} e^{-\tau_N x}}{1 - e^{i\pi u} e^{-\pi x}} dx \quad (D1)$$

where S_m has appeared in (C3) of appendix C and $\tau_j = j\pi - \pi/4$.

Consider

$$\begin{aligned} S_m(u, v, N, M) &= \sum_{j=N}^{M+N} \frac{e^{i\tau_j u} e^{-\tau_j v}}{\tau_j^{m+0.5}} = \sum_{j=N}^{M+N} \frac{e^{i\tau_j u} e^{-\tau_j v}}{(m-0.5)!} \int_0^{\infty} x^{m-0.5} e^{-\tau_j x} dx \\ &= \frac{e^{i\tau_N u} e^{-\tau_N v}}{(m-0.5)!} \int_0^{\infty} \frac{(1 - e^{iM\pi u} e^{-M\pi v} e^{-M\pi x}) x^{m-0.5} e^{-\tau_N x}}{1 - e^{i\pi u} e^{-\pi v} e^{-\pi x}} dx \end{aligned}$$

Introduce

$$R_m(u, v, M, N) = \frac{e^{i\tau_N u} e^{-\tau_N v} e^{iM\pi u} e^{-M\pi v}}{(m-0.5)!} \int_0^{\infty} \frac{x^{m-0.5} e^{-(\tau_N + M\pi)x}}{1 - e^{i\pi u} e^{-\pi v} e^{-\pi x}} dx$$

For $m \geq 1$ we have

$$|R_m(u, v, M, N)| < \frac{e^{-\tau_N v} e^{-M\pi v}}{(m-0.5)! \pi} \int_0^{\infty} x^{m-1.5} e^{-(\tau_N + M\pi)x} dx = \frac{e^{-\tau_N v} e^{-M\pi v}}{\pi (m-0.5) (\tau_N + M\pi)^{m-0.5}}$$

Thus,

$$\lim_{v \rightarrow 0} \lim_{M \rightarrow \infty} R_m(u, v, M, N) = \lim_{M \rightarrow \infty} \lim_{v \rightarrow 0} R_m(u, v, M, N) = 0$$

For $m = 0$ and when $u \neq 2n$ (n integer), there exists a δ independent of x, v ($x > 0, v > 0$) such that $|1 - e^{-i\pi u} e^{-\pi v} e^{-\pi x}| > \delta$. Thus,

$$|R_0(u, v, M, N)| < \frac{e^{-\tau_N v} e^{-M\pi v}}{\sqrt{\pi} \delta} \int_0^{\infty} \frac{e^{-(\tau_N + M\pi)x}}{\sqrt{x}} dx = \frac{e^{-\tau_N v} e^{-M\pi v}}{\delta \sqrt{\tau_N + M\pi}}$$

and

$$\lim_{v \rightarrow 0} \lim_{M \rightarrow \infty} R_0(u, v, M, N) = \lim_{M \rightarrow \infty} \lim_{v \rightarrow 0} R_0(u, v, M, N) = 0, \quad u \neq 2n$$

From this it follows

$$S_m(u, N) = \lim_{v \rightarrow 0} I_m(u, v, N)$$

where

$$I_m(u, v, N) = \frac{e^{i\tau_N u} e^{-\tau_N v}}{(m-0.5)!} \int_0^{\infty} \frac{x^{m-0.5} e^{-\tau_N x}}{1 - e^{-i\pi u} e^{-\pi v} e^{-\pi x}} dx$$

Introduce

$$I_m(u, N) = \frac{e^{i\tau_N u}}{(m-0.5)!} \int_0^{\infty} \frac{x^{m-0.5} e^{-\tau_N x}}{1 - e^{-i\pi u} e^{-\pi x}} dx \quad (D2)$$

But

$$|I_m(u, v, N) - I_m(u, N)| < \frac{1}{(m-0.5)!} \int_0^{\infty} \left| \frac{e^{-\tau_N v}}{1 - e^{-i\pi u} e^{-\pi v} e^{-\pi x}} - \frac{1}{1 - e^{-i\pi u} e^{-\pi x}} \right| \cdot x^{m-0.5} e^{-\tau_N x} dx$$

Proceeding as before one can show that

$$\lim_{v \rightarrow 0} \left| I_m(u, v, N) - I_m(u, N) \right| = 0 \text{ if } (m, u) \neq (0, 2n), n \text{ integer}$$

Thus,

$$S_m(u, N) = \lim_{v \rightarrow 0} \{ I_m(u, v, N) \} = I_m(u, N) \quad (D3)$$

which proves the statement (D1).

Appendix E

In this appendix we will investigate $S(T_\theta, \beta_\theta)$, defined by (17) in section III, in the neighborhood of its singularities.

Consider

$$I_m(u, v, N) = \frac{e^{i\tau_N u - \tau_N v}}{(m-0.5)!} \int_0^\infty \frac{x^{m-0.5} e^{-\tau_N x}}{1 - e^{i\pi u} e^{-\pi v} e^{-\pi x}} dx$$

where $u > 0$, $v > 0$ and $\tau_N = N\pi - \pi/4$, N being a positive integer and m a non-negative integer. Introducing complex notation we have

$$h(z) = \frac{z^{m-0.5} e^{\tau_N z}}{1 - e^{i\pi u} e^{-\pi v} e^{\pi z}}$$

and $h(z)$ is multi-valued, but can be made single-valued by introducing a branch-cut from the origin to infinity. Here we choose the cut along the negative real axis (see figure 12). We can then represent $I_m(u, v, N)$ by the following complex integral

$$I_m(u, v, N) = \frac{(-1)^m e^{i\tau_N u - \tau_N v}}{2i(m-0.5)!} \int_{\Gamma_1} \frac{z^{m-0.5} e^{\tau_N z}}{1 - e^{i\pi u} e^{-\pi v} e^{\pi z}} dz$$

where the path of integration, Γ_1 , is around the cut (see figure 12).

By contour deformation we have

$$I_m(u, v, N) = \frac{(-1)^m e^{i\tau_N u - \tau_N v}}{2i(m-0.5)!} \int_{\Gamma_2} \frac{z^{m-0.5} e^{\tau_N z}}{1 - e^{i\pi u} e^{-\pi v} e^{\pi z}} dz$$

and Γ_2 is parallel to the imaginary axis and $\text{Re}\{z\} < v$, $z \in \Gamma_2$ (see figure 12).

But

$$I_m(u, v, N) = I_m(u, v, 1) - B_m(u, N)$$

where

$$B_m(u, N) = \sum_{j=1}^{N-1} \frac{e^{i\tau_j u}}{\tau_j^{m+0.5}}$$

and $B_m(u, N)$ is finite for all u . $I_m(u, v, 1)$ can also be evaluated by the method of residues. Thus,

$$I_m(u, v, 1) = \sum_{k=0}^{\infty} a_k^{(m)}(u, v)$$

where

$$a_k^{(m)}(u, v) = \frac{(-1)^m \epsilon_k}{2(m-0.5)!} [(v-iu+2ik)^{m-0.5} e^{-ik\pi/2} + (v-iu-2ik)^{m-0.5} e^{ik\pi/2}]$$

and

$$\epsilon_k = \begin{cases} 1, & k = 0 \\ 2, & k \geq 1 \end{cases}$$

In the Riemann sheet under consideration we have

$$\sqrt{v-iu+2ik} = |v-iu+2ik|^{0.5} e^{i\phi_1}, \quad -\pi/4 < \phi_1 < \pi/4$$

$$\sqrt{v-iu-2ik} = |v-iu-2ik|^{0.5} e^{i\phi_2}, \quad -\pi/4 < \phi_2 < 0$$

Introduce

$$A_m(u) = \sum_{k=0}^{\infty} a_k^{(m)}(u) \quad (E1)$$

Where

$$a_k^{(m)}(u) = \frac{(-1)^m \epsilon_k}{2(m-0.5)!} \left[|u-2k|^{m-0.5} e^{-ik\pi/2} \times e^{-i(m-0.5)(\pi/2) \operatorname{sgn}(u-2k)} \right. \\ \left. + |u+2k|^{m-0.5} e^{ik\pi/2} e^{-i(m-0.5)\pi/2} \right]$$

From the mean value theorem it follows that there exists an v_k such that

$$|I_m(u, v, 1) - A_m(u)| \leq \sum_{k=0}^{\infty} |a_k^{(m)}(u, v) - a_k^{(m)}(u)| = v \sum_{k=0}^{\infty} \left| \frac{\partial a_k^{(m)}}{\partial v}(u, v_k) \right|; \quad v_k \in (0, v)$$

But

$$\lim_{v \rightarrow 0} v \sum_{k=0}^{\infty} \left| \frac{\partial a_k^{(m)}}{\partial v}(u, v_k) \right| = 0$$

except when $m = 0$ and $u = 2n$. Thus,

$$S_m(u, 1) = \lim_{v \rightarrow 0} I_m(u, v, 1) = A_m(u) \quad (E2)$$

when $m \neq 0$ or $u \neq 2n$. We notice here that $S_m(u,1)$ is finite for all u if $m \geq 1$.

In order to investigate $S_0(u,1)$ in the neighborhood of $2n$ we will use $A_0(u)$. For $|u-2n| < 1$ we have

$$A_0(u) = a^{(0)}(u) + A_0^{(n)}(u)$$

where

$$A_0^{(n)}(u) = \sum_{k \neq n} a_k^{(0)}(u)$$

and $A_0^{(n)}(u)$ is finite for $|u-2n| < 1$. Thus,

$$S_0(u,1) = \frac{e^{-in\pi/2} e^{i(\pi/4)\text{sgn}(u-2n)}}{\sqrt{\pi}|u-2n|} + A_0^{(n)}(2n) + \begin{cases} 0, & n = 0 \\ \sqrt{i/4n} e^{i\pi n/2}, & n \geq 1 \end{cases} \quad (E3)$$

where

$$\text{sgn}(x) = \begin{cases} 1, & x > 0 \\ -1, & x < 0 \end{cases}$$

Thus for $|T_0 - 2n| < 1$ we have

$$F(T_\theta, \beta_\theta, N) = \frac{i\sqrt{2i/\pi}\beta_\theta}{(1+2\beta_\theta)} S_0(T_\theta, N) = \frac{i^{n+1}\sqrt{2}\beta_\theta e^{i(\pi/2)H(u-2n)}}{\pi(1+2\beta_\theta)^{1+n}\sqrt{|T_\theta-2n|}}$$

$$+ \frac{i\sqrt{2i}\beta_\theta}{\pi(1+2\beta_\theta)^{1+n}} [A_0^{(n)}(2n) - B_0(2n, N)] + \left\{ \begin{array}{ll} 0, & n=0 \\ \sqrt{i/4n} e^{in\pi/2}, & n \geq 1 \end{array} \right\}$$

and

$$\operatorname{Re}\{F(T_\theta, \beta_\theta, N)\} = \frac{\beta_\theta}{\pi(1+2\beta_\theta)^{1+n}} [\sqrt{2/|T_\theta-2n|}] \cdot \left\{ \begin{array}{ll} -\cos n\pi/2, & u-2n > 0 \\ \sin n\pi/2, & u-2n < 0 \end{array} \right\}$$

$$+ \operatorname{Re}\{B_0(2n, N) - A_0^{(n)}(2n)\} + \operatorname{Im}\{B_0(2n, N) - A_0^{(n)}(2n)\}$$

$$- \left\{ \begin{array}{ll} 0, & n=0 \\ (2n)^{-1/2} \cos n\pi/2, & n \geq 1 \end{array} \right\}$$

Thus,

$$\lim_{T_\theta \rightarrow 4n-0} S(T_\theta, \beta_\theta) \text{ and } \lim_{T_\theta \rightarrow 4n+2+0} S(T_\theta, \beta_\theta)$$

exist but

$$\lim_{T_\theta \rightarrow 4n+0} S(T_\theta, \beta_\theta) \text{ and } \lim_{T_\theta \rightarrow 4n+2-0} S(T_\theta, \beta_\theta)$$

do not. Moreover, for $|T_\theta - 4n| \ll 1$, $T_\theta - 4n > 0$

$$S(T_\theta, \beta_\theta) \sim \frac{-(-1)^n \sqrt{2}\beta_\theta}{\pi(1+2\beta_\theta)^{1+2n}} \frac{1}{\sqrt{|T_\theta - 4n|}} \quad (E4)$$

and for $|T_\theta - 4n - 2| \ll 1$, $T_\theta - 4n - 2 > 0$

$$S(T_\theta, \beta_\theta) \sim \frac{(-1)^n \sqrt{2} \beta_\theta}{\pi (1 + 2\beta_\theta)^{2+2n}} \frac{1}{\sqrt{|T_\theta - 4n - 2|}} \quad (E5)$$

Appendix F

In this appendix we will make an asymptotic estimate for large T_θ of $P(T_\theta, \beta_\theta) = A(T_\theta, \beta_\theta) + S(T_\theta, \beta_\theta)$ defined by (17) in section III.

First, we notice that as long as $\text{Re}\{z_j\} < 0$ and $A(T_\theta, \beta_\theta)$ is a finite sum, $A(T_\theta, \beta_\theta)$ is exponentially attenuated and hence negligible compared to $R(T_\theta, \beta_\theta)$ for $T_\theta \gg 1$, where $R(T_\theta, \beta_\theta)$ is defined in (16) of section III.

To get an asymptotic estimate of $S(T_\theta, \beta_\theta)$ for $T_\theta \gg 1$ and $T_\theta \beta_\theta > 10$ we consider

$$S(T_\theta, \beta_\theta) = \sum_{k=1}^4 G_k(T_\theta, \beta_\theta) \quad (\text{F1})$$

where

$$G_1(T_\theta, \beta_\theta) = \frac{i\sqrt{2i/\pi\beta_\theta} e^{z_r T_\theta}}{1+2\beta_\theta} \sum_{j=21}^{\infty} \frac{e^{i\tau_j T_\theta}}{\sqrt{\tau_j}}$$

$$G_2(T_\theta, \beta_\theta) = \frac{i\sqrt{2i/\pi\beta_\theta} e^{z_r T_\theta}}{1+2\beta_\theta} \sum_{j=21}^{[T_\theta]} \frac{(e^{j T_\theta} - 1) e^{i\tau_j T_\theta}}{\sqrt{\tau_j}}$$

$$G_3(T_\theta, \beta_\theta) = \frac{i\sqrt{2i/\pi\beta_\theta} e^{z_r T_\theta}}{1+2\beta_\theta} \sum_{[T_\theta]+1}^{\infty} \frac{(e^{j T_\theta} - 1) e^{i\tau_j T_\theta}}{\sqrt{\tau_j}}$$

$$G_4(T_\theta, \beta_\theta) = \frac{-i\sqrt{1/(2\pi)} \beta_\theta z_r}{1+2\beta_\theta} \sum_{j=21}^{\infty} \frac{e^{z_j T_\theta}}{\tau_j^{3/2}}$$

Here, as before, $[T_\theta] \equiv N_\theta - 1$, N_θ being an integer.

But

$$G_1(T_\theta, \beta_\theta) = \frac{i\sqrt{2i/\pi\beta_\theta} e^{z_r T_\theta}}{1+2\beta_\theta} S_0(T_\theta, 21) \quad (F2)$$

where $S_0(T_\theta, N)$ has been defined in appendix C. The properties of $S_0(T_\theta, N)$ have been investigated in appendices C and E, and $S_0(T_\theta, 21)$ is bounded except at $T_\theta = 2n$, n being a nonnegative integer. Thus, for $T_\theta \gg 1$, $T_\theta \beta_\theta > 10$ and $T_\theta \neq 2n$, $G_1(T_\theta, \beta_\theta)$ is exponentially decreasing and negligible compared to $R(T_\theta, \beta_\theta)$.

Moreover,

$$|G_2(T_\theta, \beta_\theta)| < \frac{\sqrt{2}\beta_\theta e^{z_r T_\theta} [T_\theta]}{1+2\beta_\theta} \sum_{j=21}^{[T_\theta]} \frac{1+|e^{\delta_j T_\theta}|}{\sqrt{\tau_j}}$$

Let $\delta = \max_j [\text{Re}\{\delta_j\}]$. Then

$$|G_2(T_\theta, \beta_\theta)| < \frac{\sqrt{2}\beta_\theta (1+e^{\delta T_\theta}) e^{z_r T_\theta}}{1+2\beta_\theta} \int_{19.75}^{T_\theta} \frac{d\tau}{\sqrt{\tau}} = \frac{2\sqrt{2}\beta_\theta (1+e^{\delta T_\theta}) e^{z_r T_\theta}}{1+2\beta_\theta} (\sqrt{T_\theta} - \sqrt{19.75}) \quad (F3)$$

From appendix A it follows that $z_r < 0$, $z_r + \delta < 0$; hence, for $T_\theta \gg 1$ and $T_\theta \beta_\theta > 10$, $G_2(T_\theta, \beta_\theta)$ is small compared to $R(T_\theta, \beta_\theta)$.

When estimating $G_3(T_\theta, \beta_\theta)$ we use $\delta_j = i(8\tau_j)^{-1}$ and

$$G_3(T_\theta, \beta_\theta) \sim \frac{-\sqrt{2i/\pi\beta_\theta} e^{z_r T_\theta}}{8(1+2\beta_\theta)} \sum_{[T_\theta]+1}^{\infty} \frac{e^{i\tau_j T_\theta}}{\tau_j^{3/2}} = \frac{-\sqrt{2i/\pi\beta_\theta} e^{z_r T_\theta}}{8(1+2\beta_\theta)} S_1(T_\theta, [T_\theta]+1) \quad (F4)$$

where $S_1(T_\theta, N)$ has been introduced in appendix C. We recall that $S_1(T_\theta, [T_\theta]+1)$ is bounded for all $T_\theta > 0$, and thus when $T_\theta \gg 1$ and $T_\theta \beta_\theta > 10$, $G_3(T_\theta, \beta_\theta)$

is small compared to $R(T_\theta, \beta_\theta)$.

Finally, we go on to estimate G_4 :

$$|G_4(T_\theta, \beta_\theta)| \sim \frac{\beta_\theta |z_r| e^{z_o T_\theta}}{\sqrt{2\pi}(1+2\beta_\theta)} \sum_{j=21}^{\infty} \frac{1}{\tau_j^{3/2}} < \frac{2\sqrt{2/79}\beta_\theta |z_r| e^{z_o T_\theta}}{\pi(1+2\beta_\theta)} \quad (F5)$$

where $z_o = \max_j [\operatorname{Re}\{z_j\}] < 0$. Thus, for $T_\theta \gg 1$ and $T_\theta \beta_\theta > 10$, G_4 is small compared to $R(T_\theta, \beta_\theta)$.

From the above consideration it follows that $P(T_\theta, \beta_\theta)$ is negligible compared to $R(T_\theta, \beta_\theta)$ for $T_\theta \gg 1$, $T_\theta \beta_\theta > 1$ and $T_\theta \neq 2n$.

Appendix G

Here we will show that there exists a $p_r = \text{Re}\{p\} > 0$ such that $k(z)$, where $k(z) = p + z^2 I_0(z) K_0(z)$, has no zeros for $|\arg\{z\}| < \pi/2$.

It is easy to show that for any given $p_r > 0$ there exists a R such that $k(z)$ has no zeros for $|z| < R$, $|\arg\{z\}| \leq \pi/2$, and $R \rightarrow \infty$ as $p_r \rightarrow \infty$.

Now choose p_r such that we can write with arbitrary accuracy

$$k(z) = p + 0.5z + 0.5ze^{-2z} \quad , \quad |z| > R \quad , \quad |\arg\{z\}| \leq \pi/2$$

Moreover, for $R \gg 1$ there exists an $\epsilon(R)$ such that

$$k(z) = p + z/2 \quad , \quad z = Re^{i\phi} \quad , \quad \phi \in I(\epsilon) = (-\pi/2 + \epsilon, \pi/2 - \epsilon)$$

and $\epsilon \rightarrow 0$ as $R \rightarrow \infty$. From these expressions it follows that $k(z)$ has no zeros for $\arg\{z\} \in I(\epsilon)$; thus, by choosing p_r arbitrarily large $k(z)$ has no zeros for $|\arg\{z\}| < \pi/2$.

Appendix H

The sum defined by (32) of section IV will be studied in the following.

Consider the function

$$F(x,y) = \sum_{j=1}^{\infty} f(\xi_j, x, y) \quad , \quad x > 0 \quad , \quad y > 0. \quad (H1)$$

where

$$f(\xi, x, y) = \frac{J_1(x\xi)Y_1(y\xi) - J_1(y\xi)Y_1(x\xi)}{\xi J_1(\xi)Y_0^2(\xi)}$$

and ξ_j 's are the positive zeros of $J_0(\xi)$. Let $F(x,y)$ be split into two parts

$$\begin{aligned} F(x,y) &= \sum_{j=1}^{N-1} f(\xi_j, x, y) + \sum_{j=N}^{\infty} f(\xi_j, x, y) \\ &= F_1(x,y,N) + F_2(x,y,N) \end{aligned} \quad (H2)$$

We now choose N so that we can use asymptotic expressions for the Bessel functions when calculating $F_2(x,y,N)$. Also note that $F_1(x,y,N)$ is finite for all x,y considered. For $\xi \geq \xi_N$ we have

$$\begin{aligned} f(\xi, x, y) &= \frac{\sqrt{\pi/(2xy\xi)} \left[\frac{1+3/(16x^2\xi^2)}{1+1/(16\xi^2)} \right] \left[\frac{1+3/(16y^2\xi^2)}{\sin[\xi-\pi/4+3/(8\xi)]} \right]}{\sin^2[\xi-\pi/4-1/(8\xi)]} \\ &\quad \times \frac{\sin[(x-y)\xi-3(x-y)/(8xy\xi)]}{\sin^2[\xi-\pi/4-1/(8\xi)]} + O(\xi^{-7/2}) \end{aligned}$$

With $\xi_j = \tau_j + 1/(8\tau_j) + O(\tau_j^{-3})$ and $\tau_j = j\pi - \pi/4$ we have

$$\begin{aligned}
 F_2(x,y,N) &\approx \sqrt{\pi/(2xy)} \sum_{j=N}^{\infty} \frac{(-1)^{j+1}}{\sqrt{\tau_j}} \sin(x-y)\tau_j \\
 &+ \sqrt{\pi/(2xy)} \sum_{j=N}^{\infty} \frac{(-1)^{j+1}}{16\tau_j \sqrt{\tau_j}} \{ \sin(x-y)\tau_j + [2-6(x-y)/(xy)] \cos(x-y)\tau_j \} \\
 &= -\frac{1}{2} \sqrt{\pi/(xy)} [\operatorname{Re}\{S_0(x-y+1,N)\} + \operatorname{Im}\{S_0(x-y+1,N)\}] \\
 &+ \frac{\sqrt{\pi}(6x-6y-xy)}{32(xy)^{3/2}} \operatorname{Re}\{S_1(x-y+1,N)\} + \frac{3\sqrt{\pi}(xy-2x+2y)}{32(xy)^{3/2}} \operatorname{Im}\{S_1(x-y+1,N)\} \quad (H3)
 \end{aligned}$$

where

$$S_m(u,N) = \sum_{j=N}^{\infty} \frac{e^{i\tau_j u}}{\tau_j^{m+1/2}}$$

which has been introduced in appendix C. From the analysis given there it follows that $F_2(x,y,N)$ has singularities at $x-y+1 = 2n$, n being a nonnegative integer.

Appendix I

In the text we have calculated the radiation field of a resistive tubular antenna excited by a slice generator at both inside and outside wall of the antenna. In this appendix we shall consider the same problem except that the slice generator is located only at the antenna's outside wall, this case being referred to as the nonsymmetric excitation. Different excitations giving rise to the same radiation field as this nonsymmetric case are discussed in Reference 5.

Suppose

$$E_z(a_+, z) = -V\delta(z) + E_1(z) \quad (I1)$$

$$E_z(a_-, z) = E_1(z) \quad (I2)$$

Following the same procedure as in section II we have

$$\hat{E}_1(\alpha) = \frac{B(\gamma)}{A(\gamma)-1} V$$

where

$$B(\gamma) = \frac{ik_0}{\gamma} \frac{K_1(a\gamma)}{K_0(a\gamma)}$$

and

$$\hat{H}_\phi^I(\rho, \alpha) = -\frac{ik_0}{Z_0\gamma} \frac{I_1(\rho\gamma)}{I_0(a\gamma)} \frac{\beta B(\gamma)}{\beta A(\gamma)-1} V, \quad \rho < a \quad (I3)$$

$$\hat{H}_{\phi}^{III}(\rho, \alpha) = \frac{ik_0}{Z_0 \gamma} \frac{K_1(\rho \gamma)}{K_0(a \gamma)} \frac{1 - \beta C(\gamma)}{\beta A(\gamma) - 1} V, \quad \rho > a \quad (I4)$$

where

$$C(\gamma) = A(\gamma) - B(\gamma) = \frac{ik_0}{\gamma} \frac{I_1(a \gamma)}{I_0(a \gamma)}$$

Moreover

$$I(z) = \frac{aV}{Z_0} \int_C \frac{B(\gamma)}{\beta A(\gamma) - 1} e^{i\alpha z} d\alpha = \frac{k_0 a^2 V}{Z_0} \int_C \frac{\gamma K_1(a \gamma) I_0(a \gamma)}{\beta k_0 + i \gamma^2 a K_0(a \gamma) I_0(a \gamma)} e^{i\alpha z} d\alpha$$

By the saddle-point method the far field can easily be shown to be

$$H_{\phi}^{II}(r, \theta) \sim \frac{pa[\sin \theta I_0(pa \sin \theta) + \beta I_1(pa \sin \theta)] e^{-pr}}{2Z_0[\beta + pa \sin^2 \theta K_0(pa \sin \theta) I_0(pa \sin \theta)] r} \quad (I5)$$

Proceeding in the same way as in section III where the voltage of the slice generator is assumed to be a step-function in time, we get the following expression for the far field

$$\frac{Z_0 H_{\phi}(r, \theta, t)}{V_0} = \begin{cases} 0, & T_{\theta} < 0 \\ R(T_{\theta}, \beta_{\theta}) + P(T_{\theta}, \beta_{\theta}), & T_{\theta} > 0 \end{cases} \quad (I6)$$

where

$$R(T_{\theta}, \beta_{\theta}) = \int_0^{\infty} f(x, \beta_{\theta}) e^{-T_{\theta} x} dx$$

$$f(x, \beta_\theta) = \frac{1}{2} \frac{x[I_0(x) - \beta_\theta I_1(x)]I_0^2(x)e^x}{[\beta_\theta - xK_0(x)I_0(x)]^2 + \pi^2 x^2 I_0^4(x)}$$

$$P(T_\theta, \beta_\theta) = \operatorname{Re} \left\{ \sum_{j=1}^{\infty} \frac{I_0(z_j) + \beta_\theta I_1(z_j) e^{(T_\theta - 1)z_j}}{g'(z_j, \beta_\theta)} \right\}$$

Here $R(T_\theta, \beta_\theta)$ was evaluated numerically for a wide range of β_θ and T_θ .

Similarly, as in section III, we put

$$P(T_\theta, \beta_\theta) = A(T_\theta, \beta_\theta) + S(T_\theta, \beta_\theta) \quad (I7)$$

where

$$A(T_\theta, \beta_\theta) = \operatorname{Re} \left\{ \sum_{j=1}^{20} \frac{[I_0(z_j) + \beta_\theta I_1(z_j)] e^{(T_\theta - 1)z_j}}{g'(z_j, \beta_\theta)} \right\}$$

and

$$S(T_\theta, \beta_\theta) = \operatorname{Re} \left\{ \sum_{j=21}^{\infty} \frac{[I_0(z_j) + \beta_\theta I_1(z_j)] e^{(T_\theta - 1)z_j}}{g'(z_j, \beta_\theta)} \right\}$$

$A(T_\theta, \beta_\theta)$ was evaluated numerically. To obtain $S(T_\theta, \beta_\theta)$ we follow the procedure described in appendix C to get

$$\begin{aligned}
S(T_\theta, \beta_\theta) = & \frac{-\sqrt{2} \beta_\theta^2}{1+T_\theta/2} \{ \sin(\tau_{20} T_\theta + \pi/4) L_0(\tau_{22}, T_\theta) - \sin(\tau_{21} T_\theta + \pi/4) L_0(\tau_{21}, T_\theta) \\
& + (4z_r + T_\theta - 5) 8^{-1} [\sin(\tau_{21} T_\theta - \pi/4) L_1(\tau_{21}, T_\theta) - \sin(\tau_{20} T_\theta - \pi/4) L_1(\tau_{22}, T_\theta)] \\
& + [(b - (z_r - 1)/16) (T_\theta - 1) - (T_\theta - 1)^2 / 132] [\sin(\tau_{20} T_\theta + \pi/4) L_2(\tau_{22}, T_\theta) \\
& - \sin(\tau_{21} T_\theta + \pi/4) L_2(\tau_{21}, T_\theta)] + [(c + b(z_r - 1)/2) (T_\theta - 1) - (z_r - 1) (T_\theta - 1)^2 / 264 \\
& - (T_\theta - 1)^3 / 3072] [\sin(\tau_{21} T_\theta - \pi/4) L_3(\tau_{21}, T_\theta) - \sin(\tau_{20} T_\theta - \pi/4) L_3(\tau_{22}, T_\theta)] \} \\
& \quad (18)
\end{aligned}$$

For $0 < T_\theta < 20$, and

$$\begin{aligned}
s(T_\theta, \beta_\theta) &= \frac{\sqrt{2} \beta_\theta^2}{\pi(1+2\beta_\theta)} \frac{[T_\theta]}{1+T_\theta/2} \left\{ \sum_{j=21}^{[T_\theta]} \tau_j^{-1/2} \sin[(\tau_j + \Delta_j)T_\theta + \pi/4] e^{(bT_\theta)/\tau_j^2} \right. \\
&\quad - \sum_{j=21}^{[T_\theta]} \tau_j^{-3/2} / 2 (z_r - 1) \sin[(\tau_j + \Delta_j)T_\theta - \pi/4] e^{(bT_\theta)/\tau_j^2} \\
&\quad - \sin(\tau_{M_\theta} T_\theta + \pi/4) L_0(\tau_{P_\theta}, T_\theta) + \sin(\tau_{N_\theta} T_\theta + \pi/4) L_0(\tau_{N_\theta}, T_\theta) \\
&\quad - 8^{-1} (4z_r + T_\theta - 5) [\sin(\tau_{N_\theta} T_\theta - \pi/4) L_1(\tau_{N_\theta}, T_\theta) - \sin(\tau_{M_\theta} T_\theta - \pi/4) L_1(\tau_{P_\theta}, T_\theta)] \\
&\quad - [\{b - (z_r - 1)/16\} (T_\theta - 1) - (T_\theta - 1)^2 / 132] [\sin(\tau_{M_\theta} T_\theta + \pi/4) L_2(\tau_{P_\theta}, T_\theta) \\
&\quad - \sin(\tau_{N_\theta} T_\theta + \pi/4) L_2(\tau_{N_\theta}, T_\theta)] - [\{c + b(z_r - 1)/2\} (T_\theta - 1) - (z_r - 1)(T_\theta - 1)^2 / 264 \\
&\quad - (T_\theta - 1)^3 / 3072] [\sin(\tau_{N_\theta} T_\theta - \pi/4) L_3(\tau_{N_\theta}, T_\theta) - \sin(\tau_{M_\theta} T_\theta - \pi/4) L_3(\tau_{P_\theta}, T_\theta)] \} \\
&\hspace{15em} (I9)
\end{aligned}$$

for $T_\theta > 20$.

The quantities appearing in (I8) and (I9) have been defined in appendices B and C.

Following the procedure as described in appendix E we see that for n being a nonnegative integer, $\lim_{T_\theta \rightarrow 4n-0} S(T_\theta, \beta_\theta)$ and $\lim_{T_\theta \rightarrow 4n+2+0} S(T_\theta, \beta_\theta)$ exist but $\lim_{T_\theta \rightarrow 4n+0} S(T_\theta, \beta_\theta)$ and $\lim_{T_\theta \rightarrow 4n+2-0} S(T_\theta, \beta_\theta)$ do not. Moreover, for $|T_\theta - 4n| \ll 1$, $T_\theta - 4n > 0$

$$S(T_\theta, \beta_\theta) \sim \frac{(-1)^{n\sqrt{2}} \beta_\theta^2}{\pi (1+2\beta_\theta)^{1+2n}} \frac{1}{\sqrt{|T_\theta - 4n|}} \quad (\text{I10})$$

and for $|T_\theta - 4n - 2| \ll 1$, $T_\theta - 4n - 2 < 0$

$$S(T_\theta, \beta_\theta) \sim \frac{-(-1)^{n\sqrt{2}} \beta_\theta^2}{\pi (1+2\beta_\theta)^{2+2n}} \frac{1}{\sqrt{|T_\theta - 4n - 2|}} \quad (\text{I11})$$

For $T_\theta \ll 1$ we have [see (I8)] $R(T_\theta, \beta_\theta) \sim (1-\beta_\theta)(2T_\theta\pi^2)^{-\frac{1}{2}}$. Thus,

$$\frac{\rho Z_o H_\phi}{V_o} \sim \frac{1+\beta_\theta}{\pi\sqrt{2}(1+2\beta_\theta)} \frac{1}{\sqrt{T_\theta}} \quad \text{when } T_\theta \rightarrow 0 \quad (\text{I12})$$

Using the method described on page 10 when estimating $R(T_\theta, \beta_\theta)$ for $T_\theta \beta_\theta \gg 1$ we get

$$R(T_\theta, \beta_\theta) \sim \frac{1}{2\beta_\theta^2 T_\theta^2} \left[1 - \frac{\beta_\theta}{T_\theta} + \frac{2}{T_\theta} + \frac{4}{\beta_\theta T_\theta} \ln \frac{2T_\theta}{\Gamma} - \frac{2n}{\beta_\theta T_\theta} \right] \quad (\text{I13})$$

Moreover, for $T_\theta \gg 1$, $\beta_\theta T_\theta > 10$ and $T_\theta \neq 2n$, $P(T_\theta, \beta_\theta)$ is small compared to $R(T_\theta, \beta_\theta)$ (see appendix F for the proof). Thus, asymptotically we have

$$\frac{\rho Z_o H_\phi}{V_o} \sim R(T_\theta, \beta_\theta)$$

where $R(T_\theta, \beta_\theta)$ is given by (I13).

For $\beta_\theta \gg 1$ we have asymptotically

$$\frac{\rho Z_o H_\phi(\rho, z, t)}{V_o} \sim h_1(T_\theta) + \beta_\theta^{-1}[h_2(T_\theta) + h_3(T_\theta)] + O(\beta_\theta^{-2}) \quad (I14)$$

where

$$h_1(T_\theta) = \frac{1}{4\pi i} \int_{L_1} I_1(\zeta) e^{q_\theta \zeta} d\zeta$$

$$= -\frac{1}{2\pi} \int_0^\infty J_1(y) \sin(q_\theta y) dy = \begin{cases} (1-T_\theta)/(2\pi\sqrt{2T_\theta-T_\theta^2}), & 0 < T_\theta < 2 \\ 0, & T_\theta > 2 \end{cases}$$

$$h_2(T_\theta) = \frac{1}{4\pi i} \int_{L_1} I_o(\zeta) e^{q_\theta \zeta} d\zeta = \begin{cases} 1/(2\pi\sqrt{2T_\theta-T_\theta^2}), & 0 < T_\theta < 2 \\ 0, & T_\theta > 2 \end{cases}$$

and

$$h_3(T_\theta) = -\frac{1}{4\pi i} \int_{L_1} \zeta I_1(\zeta) I_o(\zeta) K_o(\zeta) e^{q_\theta \zeta} d\zeta$$

$$= \begin{cases} \frac{1}{\pi} \int_0^\infty x I_o(x) K_1(x) K_o(x) \cosh[(T_\theta-1)x] dx, & 0 < T_\theta < 2 \\ \frac{1}{2\pi^2} \int_0^\infty K_o(x) e^{-(T_\theta-1)x} dx + \frac{3}{2\pi^2} \int_0^\infty x I_1(x) I_o(x) K_o(x) e^{-(T_\theta-1)x} dx, & 2 < T_\theta < 4 \\ -\frac{1}{2} \int_0^\infty x I_o^2(x) I_1(x) e^{-(T_\theta-1)x} dx, & T_\theta > 4 \end{cases}$$

Equation (I8) is graphed in figure 13 for $T_\theta < 12$. Comparing this figure with figure 6 we see that, for $T_\theta < 10$, there is a significant difference in the radiation field between the symmetric and the nonsymmetric case. However, for $T_\theta > 15$ and $\beta_\theta < 1$ the radiation field of the two cases is largely the same except near the singularities at $T_\theta = 2n$; for $T_\theta > 15$ and $\beta_\theta > 1$ the radiation field of the nonsymmetric case is slightly weaker than that of the symmetric case.

Following the procedure in section IV we obtain for the near field

$$\begin{aligned}
\frac{Z_0}{V_0} H_\phi(\rho, z, t) &= f_1(\rho, z, t) \\
&= \frac{1}{2\pi i} \int_{\Gamma_\gamma} a\gamma K_1(\rho\gamma) d\gamma \frac{1}{2\pi i} \int_{C_p} \frac{[\gamma I_0(a\gamma) + \beta p I_1(a\gamma)] e^{pct} e^{-z\sqrt{p^2 - \gamma^2}}}{[\beta p + a\gamma^2 I_0(a\gamma) K_0(a\gamma)] \sqrt{p^2 - \gamma^2}} dp \\
&= f(\rho, z, t) + \frac{1}{2\pi i} \int_{\Gamma_\gamma} a\beta\gamma K_1(\rho\gamma) I_1(a\gamma) d\gamma \\
&\quad \times \frac{1}{2\pi i} \int_{C_p} \frac{p e^{pct} e^{-z\sqrt{p^2 - z^2}}}{[\beta p + a\gamma^2 I_0(a\gamma) K_0(a\gamma)] \sqrt{p^2 - \gamma^2}} dp \tag{I15}
\end{aligned}$$

For β small we expand this expression in power series of β and keep terms up to order β . Thus,

$$f_1(\rho, z, t) \approx f_0(\rho, z, t) + k_1(\rho, z, t) + k_2(\rho, z, t) \tag{I16}$$

where f_0 and k_1 have been defined in section IV, and

$$k_2(\rho, z, t) = \begin{cases} 0 & , \quad \lambda < \rho - a \\ \frac{\beta ct}{\lambda} \frac{1}{2\pi i} \int_{\Gamma_Y} \frac{K_1(\rho\gamma) I_1(a\gamma) I_1(\lambda\gamma)}{I_0(a\gamma) K_0(a\gamma)} d\gamma & , \quad \lambda > \rho - a \end{cases}$$

For $\lambda > \rho - a$ the integral can be deformed as follows:

$$\begin{aligned} k_2(\rho, z, t) &= \frac{\beta ct}{2\pi\lambda} \left\{ \int_{\Gamma'} \frac{K_1(\rho\gamma) I_1(a\gamma) K_1(\lambda\gamma)}{I_0(a\gamma) K_0(a\gamma)} d\gamma - \int_{\Gamma''} \frac{K_1(\rho\gamma) I_1(a\gamma) K_1(\lambda\gamma)}{I_0(a\gamma) K_0(a\gamma)} d\gamma \right. \\ &\quad \left. + \int_{\Gamma'} \frac{K_1(\rho\gamma) I_1(a\gamma) K_1(\lambda\gamma e^{i\pi})}{I_0(a\gamma) K_0(a\gamma)} d\gamma - \int_{\Gamma''} \frac{K_1(\rho\gamma) I_1(a\gamma) K_1(\lambda\gamma e^{-i\pi})}{I_0(a\gamma) K_0(a\gamma)} d\gamma \right\} \\ &= - \frac{\beta ct}{a\lambda} \int_0^\infty \frac{K_1(\sigma\lambda/a) I_1(\sigma) [I_1(\sigma\rho/a) K_0(\sigma) + K_1(\sigma\rho/a) I_0(\sigma)]}{K_0(\sigma) [K_0^2(\sigma) + \pi^2 I_0^2(\sigma)]} d\sigma \\ &\quad + \frac{2\beta ct}{\pi a\lambda} \sum_{j=1}^{\infty} \frac{J_1(\xi_j \rho/a) J_1(\xi_j \lambda/a) - Y_1(\xi_j \rho/a) Y_1(\xi_j \lambda/a)}{Y_0(\xi_j)} \end{aligned} \quad (I17)$$

From the above expressions it is easy to show that $k_1 + k_2$ is finite for $\lambda > \rho - a$. Thus, up to order of βf_1 is finite except at $ct = \sqrt{(\rho - a)^2 + z^2}$. It is not surprising that f_1 is finite in this approximation because the singularities in the exact form of f_1 appear only in terms of order β^2 and higher in the power series expansion (I16).

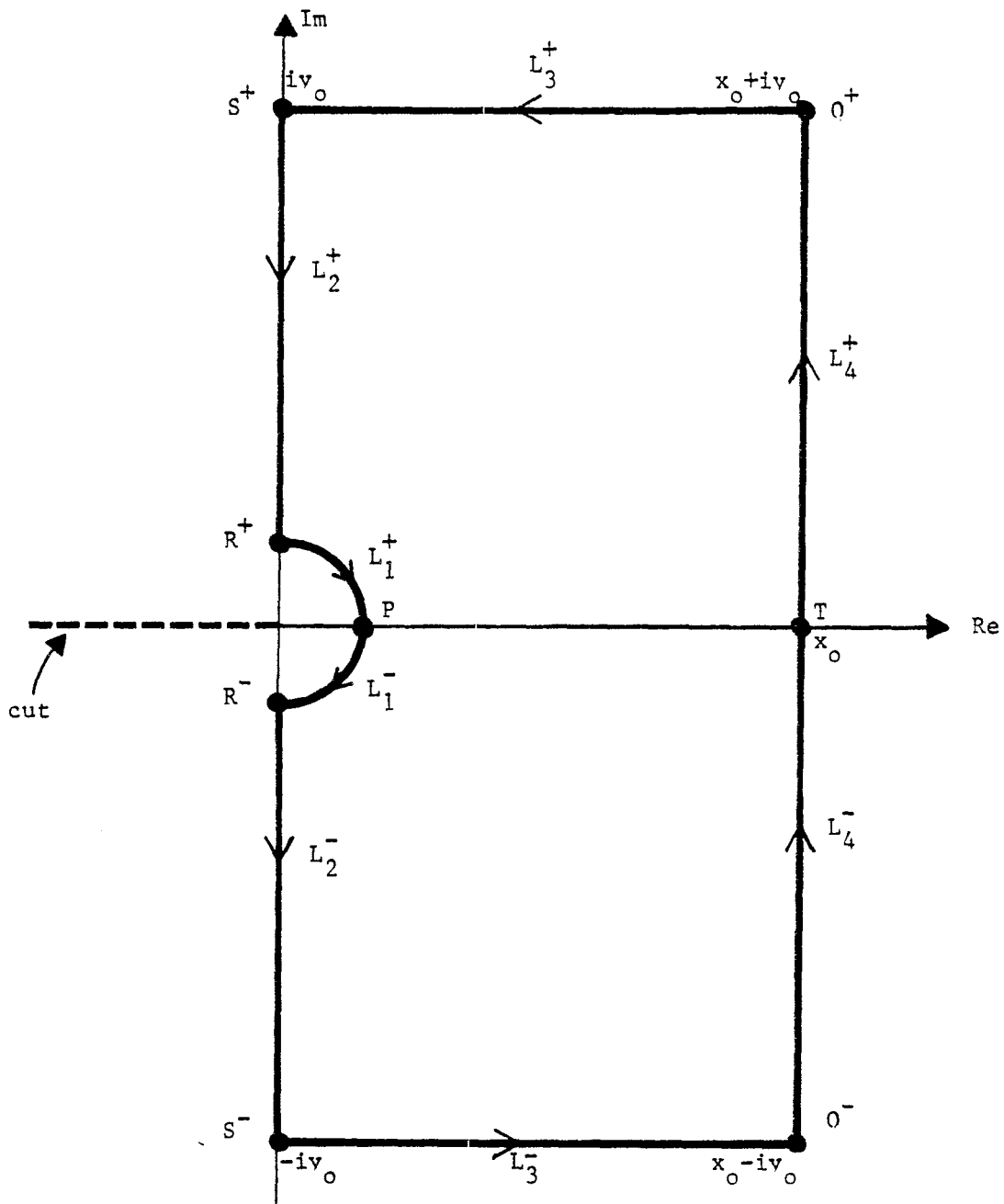


Figure 11. The path L in appendix A.

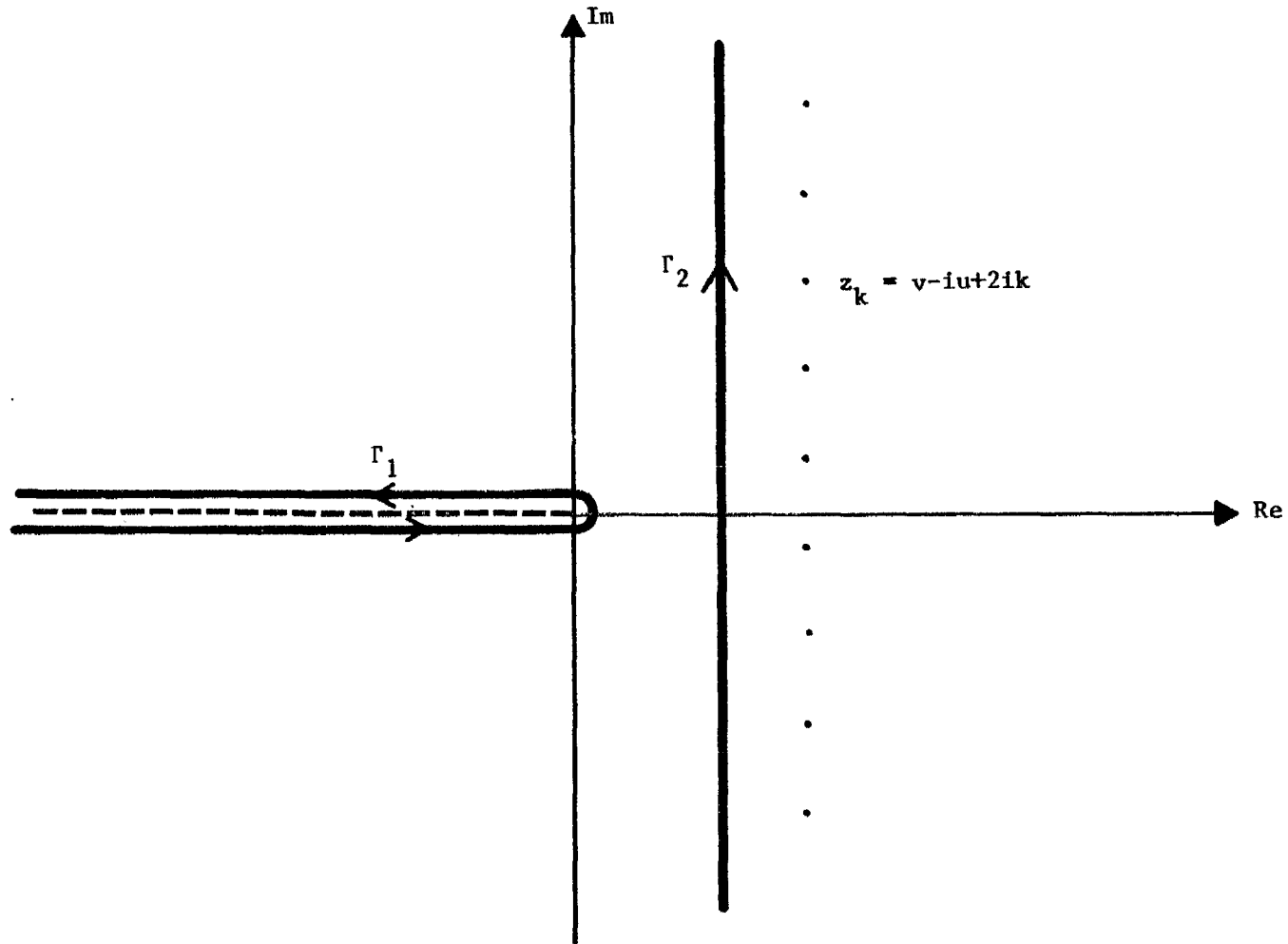


Figure 12. The paths of integration in appendix E.

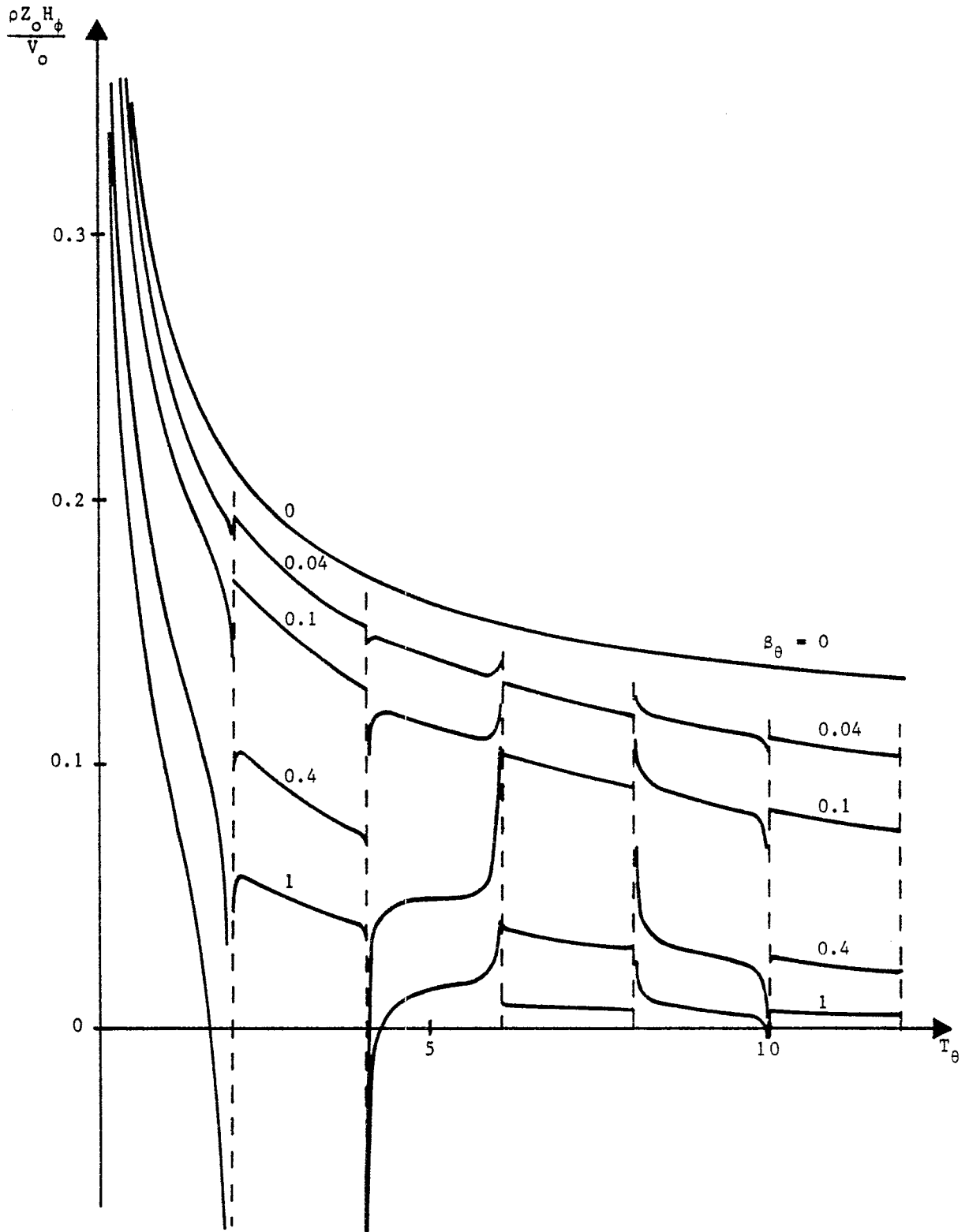


Figure 13. Radiation field for a step-function voltage from the nonsymmetrically excited antenna in appendix I.

Acknowledgment

We wish to thank Capt. Carl Baum for his suggestions, Dr. Kelvin Lee for his criticism of the manuscript, Mr. Dick Sassman for his numerical computations and Mrs. Georgene Peralta for typing the note.

References

1. R. W. Latham and K. S. H. Lee, "Pulse radiation and synthesis by an infinite cylindrical antenna," *Sensor and Simulation Note* 73, February 1969.
2. R. W. Latham and K. S. H. Lee, "Radiation of an infinite cylindrical antenna with uniform resistive loading," *Sensor and Simulation Note* 83, April 1969.
3. R. W. Latham and K. S. H. Lee, "Waveforms near a cylindrical antenna," *Sensor and Simulation Note* 89, June 1969.
4. P. O. Brundell, "Transient electromagnetic waves around a cylindrical transmitting antenna," *Ericsson Technics*, Sweden, Vol. 16, No. 1, pp. 137-162, 1960.
5. R. W. P. King and T. T. Wu, "The thick tubular transmitting antenna," *Radio Science*, Vol. 2, No. 9, pp. 1061-1065.
6. R. E. Collin and F. J. Zucker, Antenna Theory, McGraw-Hill, New York, Chapter 8, 1969.
7. G. N. Watson, Theory of Bessel Functions, Cambridge University Press, Cambridge, Second Edition, 1944.
8. W. Magnus, F. Oberhettinger and R. P. Soni, Formulas and Theorems for the Special Functions of Mathematical Physics, Springer-Verlag, New York, 1966.